

 M 2020

U. PORTO
FEUP FACULDADE DE ENGENHARIA
UNIVERSIDADE DO PORTO

TREATMENT OF WASTEWATER GENERATED BY OLIVE OIL PRODUCTION USING THE HETEROGENEOUS FENTON PROCESS

MARIA JOÃO COUTO FERNANDES CARNEIRO
MASTER DISSERTATION PRESENTED
TO FACULDADE DE ENGENHARIA DA UNIVERSIDADE DO PORTO IN
ENGENHARIA QUÍMICA

Master's in chemical engineering

***Treatment of wastewater generated in olive oil
production using the heterogeneous Fenton
process***

Master dissertation

of

Maria João Couto Fernandes Carneiro

Developed within the course of dissertation

held in

LEPABE - Laboratory for Process Engineering, Environment, Biotechnology and Energy

in collaboration with

Laboratory of Separation and Reaction Engineering - Laboratory of Catalysis and Materials



Supervisor: Professor Luís Miguel Palma Madeira

Co-supervisor: Professor Adrián Manuel Tavares da Silva



March 2021

Acknowledgments

I would like to acknowledge to the Faculty of Engineering of the University of Porto (FEUP), Department of Chemical Engineering (DEQ) and Laboratory for Process Engineering, Environment, Biotechnology and Energy (LEPABE) for the resources and facilities to develop my work.

I want to acknowledge my supervisor, Professor Miguel Madeira, and co-supervisor, Professor Adrián Tavares da Silva, for the opportunity of developing this important theme. Additionally, I want to acknowledge to Engenheiro Bruno Esteves for his guidance, encouragement, and availability throughout the last six months. Also, I would like to acknowledge the entire lab team of E-146 for the help, and companionship while developing this master dissertation.

I want to specially acknowledge to my parents, family, and friends, particularly Pedro Castro, Cláudia Martins, Inês Marques, Ivan Strugov, Rui Azevedo and Luísa Azevedo, for their support, patience and friendship through the last months.

This work was financially supported by: Base funding - UIDB/00511/2020 of the Laboratory for Process Engineering, Environment, Biotechnology and Energy - LEPABE - funded by national funds through the FCT/MCTES (PIDDAC), and project NORTE-01-0247-FEDER-39789 funded by European Regional Development Funds (ERDF) through North Portugal Regional Operational Programme (NORTE 2020).

Professor Adrián Manuel Tavares da Silva, co-supervisor of this work, is member of the Associate Laboratory LSRE-LCM funded by national funds through FCT/MCTES (PIDDAC): Base Funding UIDB/50020/2020.



Abstract

Water is an essential natural resource for life and the natural ecosystem; however, its increasing demand due to industrialization has put this essential resource at jeopardy. Olive oil production is one of the industrial activities contributing to this threat due to the discharges of olive mill wastewater (OMW), characterized by a high organic load and resulting in high levels of toxicity. Different strategies have been applied to handle this problem. The first approach consists in the pre-treatment of these wastewaters; however, OMW still presents a high level of toxicity after this stage. Thus, other solutions have been applied, namely the advanced oxidation processes (AOPs). These processes are highly efficient, safe, and inexpensive in some cases, making them an interesting choice for wastewater treatment. AOPs are based on the production of highly reactive hydroxyl radicals (HO^\bullet) responsible for the mineralization of the organic compounds. One typical example is the Fenton process, where hydrogen peroxide (H_2O_2) and dissolved iron (Fe^{2+}) are used to produce the highly reactive radicals under near room conditions of temperature and atmospheric pressure. However, the use of high loads of iron and the production of iron sludge are some limitations of this process. To overcome these drawbacks, a new perspective is adopted comprising the use of solid catalysts, known as the heterogeneous Fenton or Fenton-like process. In the present work, iron-based activated carbons prepared from olive residues (OSAC-Fe) were employed as solid catalysts to treat a synthetic solution and a real OMW. The total phenolic content (TPh), the mineralization level (removal of total organic carbon - TOC), oxidant consumption, removal of chemical oxygen demand (COD), and iron leached were investigated. Throughout the work, it was concluded that catalysts with particle sizes ranging $0.80 < d_p < 1.0$ mm with catalyst and H_2O_2 concentrations of 0.5 g L^{-1} provided the best results for both synthetic and real OMW. Actually, 11 % and 57 % of TOC and TPh removals, 24 % of H_2O_2 consumption and only 1.4 % of iron leached were obtained when using synthetic solutions after 360 min of reaction. In the case of real OMW, 8 % of TOC and 56 % of TPh removals, 45 % of H_2O_2 consumption and 20 % of COD removal were achieved after the same period of treatment. It was also concluded that the increase of temperature positively impacted the process performance where it was obtained 41 % and 93 % of TOC and TPh removals, 95 % of H_2O_2 consumption and 58 % of COD removal after 120 min only, at 75°C . Enlightened by these results, it can be said that OSAC-Fe catalysts are stable, being an efficient, greener and inexpensive strategy to handle OMW effluents.

Keywords: Olive mill wastewater, Advanced oxidation processes, Heterogeneous Fenton, Olive stone activated carbons.

Resumo

A água é um recurso essencial para a vida e para o ecossistema; porém o aumento da sua procura devido à industrialização coloca este bem essencial em risco. A produção de azeite é uma das principais indústrias que contribui para este efeito devido às suas descargas (OMW - *olive mill wastewater*), caracterizadas por um elevado conteúdo orgânico e altos níveis de toxicidade. Várias estratégias têm sido aplicadas para lidar com este problema. Uma primeira abordagem consiste no seu pré-tratamento, contudo os efluentes finais ainda apresentam toxicidade. Assim, outras estratégias têm sido aplicadas, nomeadamente os processos de oxidação avançados (POAs). Estes são altamente eficientes, seguros e económicos, tornando-os a escolha mais apropriada para o tratamento de efluentes. Os POAs baseiam-se na produção de radicais com elevado poder oxidativo (HO^{\bullet}) responsáveis pela mineralização dos compostos orgânicos. Um dos exemplos mais notório é o processo Fenton homogéneo onde o agente oxidante (H_2O_2) e uma solução de ferro (Fe^{2+}) são usados para gerar os radicais hidroxilo a pressão e temperatura ambientes. No entanto, o uso de elevadas concentrações de ferro e consequente produção de lamas são algumas das limitações deste processo. Para ultrapassar estes inconvenientes tem sido utilizada uma estratégia alternativa que se baseia na utilização de catalisadores sólidos, conhecido como processo Fenton heterogéneo. Neste trabalho foram utilizados carvões ativadas provenientes de resíduos de oliveiras e posteriormente impregnados com ferro (OSAC-Fe) para se obterem catalisadores para o tratamento de soluções sintéticas e efluentes reais. Foi analisado o conteúdo fenólico (TPh), a mineralização de compostos orgânicos (TOC), o consumo de oxidante, a remoção de carbono orgânico (COD) e o ferro lixiviado. Ao longo do trabalho concluiu-se que o tamanho de partícula de catalisador apropriado é $1,0 < d_p < 0,80$ mm usando concentrações de catalisador e H_2O_2 iguais a $0,5 \text{ g L}^{-1}$ visto que forneceram os melhores resultados para os efluentes sintéticos e reais. Obteve-se 11 % e 57 % de remoção de TOC e TPh, respetivamente, 24 % de consumo de H_2O_2 e 1,4 % de ferro lixiviado utilizando soluções sintéticas durante 360 minutos de reação. No caso do efluente real, obtiveram-se remoções de TOC e TPh de 8 e 56 %, respetivamente, 45 % de consumo de H_2O_2 e 20 % de remoção de COD para o mesmo tempo de reação. Também se concluiu que o aumento de temperatura demonstrou um impacto positivo na reação, obtendo-se 93 % de remoção de TPh, 95 % de consumo de H_2O_2 e 58 % de remoção de COD ao fim de 120 minutos de reação a $T = 75 \text{ }^{\circ}\text{C}$. Tendo em conta os resultados obtidos pode-se dizer que os catalisadores OSAC-Fe são estáveis, sendo uma estratégia eficiente, ecológica e económica para o tratamento de OMW.

Palavras-Chave: Efluentes, Processos Oxidação Avançados, Fenton Heterogéneo

Declaration

I hereby declare, under word of honour, that this work is original and that all non-original contributions are indicated, and due reference is given to the author and source

March 3, 2021

Maria João Carneiro

(Maria João Carneiro)

Index

1	Introduction.....	9
1.1	Framing and Presentation of the work.....	9
1.2	Contribution of the author	10
1.3	Organization of the thesis	11
2	Context and State-of-the-art	12
2.1	OMW's pollutants and environmental impacts of olive oil effluents.....	13
2.2	Physical-chemical processes for OMW treatment	15
2.3	The Fenton process	17
2.4	Parameters of influence on the Fenton's process	19
2.4.1	pH	19
2.4.2	Temperature.....	19
2.4.3	H ₂ O ₂ concentration	20
2.4.4	Catalyst load.....	20
2.5	Heterogeneous Fenton process or Fenton-like reactions.....	21
2.6	Activated carbons as catalysts in the heterogonous Fenton process.....	22
3	Materials and Methods	24
3.1	Catalysts preparation	24
3.2	Synthetic and real OMW composition and experimental procedure.....	24
3.3	Analytical techniques.....	27
4	Results and discussion	29
4.1.1	Influence of catalyst's particle size	29
4.1.2	Influence of the solution's composition	33
4.1.3	Influence of the catalyst concentration	35
4.2	Real Olive Mill Wastewater Treatment	38
4.2.1	Effect of catalyst load.....	38
4.2.2	Effect of temperature	40

4.2.3	Catalyst reutilization	43
5	Conclusions	44
6	Assessment of the work done	45
6.1	Objectives Achieved	45
6.2	Final Assessment	45
7	References	46
	Appendix A	51
A.1	Phenolic compounds calibration curves	51
A.2	H ₂ O ₂ solution and calibration curve	53
A.3	Folin-Ciocalteu method	54
A.4	COD measurements: H ₂ O ₂ interference	55
A.5	Iron weight percentage and Fe leaching (%)	56
	Appendix B - TPh, TOC removals and H ₂ O ₂ consumption for synthetic solutions .	58
B.1	Influence of catalyst's particle size.....	58
B.2	Influence of solution's composition	59
B.3	Influence of catalyst load	59
	Appendix C - TPh, TOC, COD removals and H ₂ O ₂ consumption for real olive mill wastewaters.....	61
C.1	Influence of catalyst load.....	61
C.2	Influence of temperature.....	62

List of Figures

- Figure 2.1** Overall scheme of the processes used for olive oil extraction: (a) 2-phase and (b) 3-phase centrifugation (adapted from Amor, C. et al., *Water*, 11 (2019) 5-29; Domingues, E. et al., *Journal of Water Process Engineering*, 39 (2021), 8)..... 12
- Figure 2.2** SEM images of an AC surface at different magnifications, the scale corresponding to the reference lengths: (a) 200 μm , (b) 100 μm , and (c) 3 μm (adapted from Barroso-Bogeat et al. 2020)..... 22
- Figure 4.1** Removal of each phenolic compound (C/C_0) over time during the catalytic process using catalysts with different particle sizes (d_p) (a) $0.80 < d_p < 1.0$ mm, (b) $0.45 < d_p < 0.80$ mm, and (c) $d_p < 0.25$ mm. Experimental conditions: SYNTHETIC-1 solution, $[\text{CAT}] = 0.5 \text{ g L}^{-1}$, $[\text{H}_2\text{O}_2] = 0.5 \text{ g L}^{-1}$, $T = 25 \text{ }^\circ\text{C}$, and $\text{pH} = 3.6$ 30
- Figure 4.2** Dimensionless concentration of all phenolic compounds (C/C_0) during the adsorption and catalytic processes using catalysts with different particle sizes (d_p). Experimental conditions: SYNTHETIC-1 solution, $[\text{CAT}] = 0.5 \text{ g L}^{-1}$, $[\text{H}_2\text{O}_2] = 0.5 \text{ g L}^{-1}$, $T = 25 \text{ }^\circ\text{C}$, and $\text{pH} = 3.6$ 31
- Figure 4.3** (a) Consumption of oxidant and (b) TOC removal during catalysis using catalysts with different particle sizes (d_p). Experimental conditions: SYNTHETIC-1 solution, $[\text{CAT}] = 0.5 \text{ g L}^{-1}$, $[\text{H}_2\text{O}_2] = 0.5 \text{ g L}^{-1}$, $T = 25 \text{ }^\circ\text{C}$, and $\text{pH} = 3.6$ 32
- Figure 4.4** Removal of TOC and phenolic compounds (TPh) (%), H_2O_2 consumption (%), and Fe leaching (wt.%) after 180 min of adsorption and 180 min of catalysis. Experimental conditions: SYNTHETIC-1 solution, $[\text{CAT}] = 0.5 \text{ g L}^{-1}$, $[\text{H}_2\text{O}_2] = 0.5 \text{ g L}^{-1}$, $T = 25 \text{ }^\circ\text{C}$, and $\text{pH} = 3.6$. Error bars were obtained from the standard errors for a confidence level of 95 %..... 32
- Figure 4.5** Dimensionless concentration of all phenolic compounds (C/C_0) during the adsorption and catalytic processes using different solution's compositions. Experimental conditions: $0.80 < d_p < 1.0$ mm, $[\text{CAT}] = 0.5 \text{ g L}^{-1}$, $[\text{H}_2\text{O}_2] = 0.5 \text{ g L}^{-1}$, $T = 25 \text{ }^\circ\text{C}$, and $\text{pH} = 3.6 - 3.8$ 33
- Figure 4.6** Removal of the individual phenolic compounds (C/C_0) over time using different solution's compositions (a) SYNTHETIC-1, (b) SYNTHETIC-2, (c) SYNTHETIC-3. Experimental conditions: $0.80 < d_p < 1.0$ mm, $[\text{CAT}] = 0.5 \text{ g L}^{-1}$, $[\text{H}_2\text{O}_2] = 0.5 \text{ g L}^{-1}$, $T = 25 \text{ }^\circ\text{C}$, and $\text{pH} = 3.6 - 3.8$ 34
- Figure 4.7** Removal of TOC and phenolic compounds (TPh) (%), H_2O_2 consumption (%), and Fe leaching (wt.%) after 180 min of adsorption and 180 min of catalysis. Experimental conditions: $0.80 < d_p < 1.0$ mm, $[\text{CAT}] = 0.5 \text{ g L}^{-1}$, $[\text{H}_2\text{O}_2] = 0.5 \text{ g L}^{-1}$, $T = 25 \text{ }^\circ\text{C}$, and $\text{pH} = 3.6 - 3.8$. Errors bars were obtained from the standard errors for a confidence level of 95 %..... 35

Figure 4.8 Dimensionless concentration of all phenolic compounds (C/C_0) during the adsorption and catalytic processes using different catalyst concentrations. Experimental conditions: SYNTHETIC-1 solution, $0.80 < d_p < 1.0$ mm, $[H_2O_2] = 0.5$ g L⁻¹, $T = 25$ °C, and $pH = 3.6$. For $[CAT] = 2.5$ g L⁻¹, catalysis starts at $t = 240$ min. 36

Figure 4.9 (a) Consumption of oxidant and **(b)** TOC removal during the catalytic process using different catalyst concentrations. Experimental conditions: SYNTHETIC-1 solution, $0.80 < d_p < 1.0$ mm, $[H_2O_2] = 0.5$ g L⁻¹, $T = 25$ °C, and $pH = 3.6$. For $[CAT] = 2.5$ g L⁻¹, catalysis starts at $t = 240$ min. 37

Figure 4.10 Removal of TOC and phenolic compounds (TPh) (%), H₂O₂ consumption (%), and Fe leaching (wt.%) after 180/240 min of adsorption + 180/120 min of catalysis. Experimental conditions: SYNTHETIC-1 solution, $0.80 < d_p < 1.0$ mm, $[H_2O_2] = 0.5$ g L⁻¹, $T = 25$ °C, and $pH = 3.6$. Errors bars were obtained from the standard errors for a confidence level of 95 %. For $[CAT] = 2.5$ g L⁻¹, the catalytic process starts at $t = 240$ min. 38

Figure 4.11 (a) TPh removal **(b)** Consumption of oxidant and **(c)** TOC removal in real effluents using different concentrations of catalyst. Experimental conditions: $0.80 < d_p < 1.0$ mm, $[H_2O_2] = 0.5$ g L⁻¹, $T = 24$ °C, $pH = 3.4$ 39

Figure 4.12 Removal of TOC, phenolic compounds (TPh), COD (%) and H₂O₂ consumption (%) in real effluents using different catalyst concentrations. Experimental conditions: $0.80 < d_p < 1.0$ mm, $[H_2O_2] = 0.5$ g L⁻¹, $T = 24$ °C, $pH = 3.4$. Errors bars were obtained from the standard errors for a confidence level of 95 %. 40

Figure 4.13 (a) TPh removal **(b)** consumption of oxidant and **(c)** TOC removal in real effluents at different temperatures. Experimental conditions: $0.80 < d_p < 1.0$ mm, $[CAT] = 0.5$ g L⁻¹, $[H_2O_2] = 0.5$ g L⁻¹, $pH = 3.4$. Catalytic results ended at $t = 270$ min using $T = 50$ °C and ended at 120 min for $T = 75$ °C. 41

Figure 4.14 Removal of TOC, phenolic compounds (TPh) and COD (%), H₂O₂ consumption (%) in real effluents at different temperatures. Experimental conditions: $0.80 < d_p < 1.0$ mm, $[CAT] = 0.5$ g L⁻¹, $[H_2O_2] = 0.5$ g L⁻¹, $pH = 3.4$. Errors bars were obtained from the standard errors for a confidence level of 95 %. 42

Figure 4.15 Removal of phenolic compounds (TPh), COD (%) and H₂O₂ consumption (%) in 4 consecutive cycles using a real effluent. Experimental conditions: $0.80 < d_p < 1.0$ mm, $[CAT] = 0.5$ g L⁻¹, $[H_2O_2] = 0.5$ g L⁻¹, $pH = 3.4$. CYCLE-1 ends at 120 min, the remained cycles ended at 180 min. Errors bars were obtained from the standard errors for a confidence level of 95 %. 43

Figure A.1 Calibration curves for **(a)** gallic acid and **(b)** tyrosol. 51

Figure A.2 Calibration curve for **(a)** 4-hydroxybenzoic acid and **(b)** protocatechuic acid. 51

Figure A.3 Calibration curve for **(a)** caffeic acid and **(b)** vanillic acid. 52

Figure A.4 Calibration curve for (a) syringic acid and (b) veratric acid.	52
Figure A.5 Calibration curve of H_2O_2 at 400 nm for different concentrations.	53
Figure A.6 Calibration curve for the Folin-Ciocalteu method.	54
Figure A.7 Calibration curve for COD measures at 620 nm with H_2O_2 discount.	55
Figure B.1 Removal of phenolic compounds (C/C_0) over time during the adsorption process using catalysts with different particle sizes (d_p) (a) $0.80 < d_p < 1.0$ mm, (b) $0.45 < d_p < 0.80$ mm, and (c) $d_p < 0.25$ mm. Experimental conditions: SYNTHETIC-1 solution, $[CAT] = 0.5$ g L^{-1} , $[H_2O_2] = 0.5$ g L^{-1} , $T = 25$ °C, and $pH = 3.6$	58
Figure B.2 a) Consumption of oxidant and (b) TOC removal during the catalytic process using different solution's compositions. Experimental conditions: $[CAT] = 0.5$ g L^{-1} , $0.80 < d_p < 1.0$ mm, $[H_2O_2] = 0.5$ g L^{-1} , $T = 25$ °C, and $pH = 3.6 - 3.8$	59
Figure B.3 Removal of phenolic compounds over time using different catalyst concentrations. Experimental conditions: SYNTHETIC-1 solution, $0.80 < d_p < 1.0$ mm, $[H_2O_2] = 0.5$ g L^{-1} , $T = 25$ °C, and $pH = 3.6$	60

List of Tables

Table 2.1 Physico-chemical properties of OMW using different processes (adapted from (Babić et al., 2019; Domingues et al., 2021; Nieto et al., 2011a).	14
Table 2.2 Physico-chemical parameters for water consumption with Recommendable values (VMR) in Portugal and Emission Limit Values (ELV) of residual waters in Porto (adapted from (Diário da República, 1998; SIMDOURO-Grupo Águas de Portugal, n.d.)).	14
Table 2.3 Coagulation-flocculation processes as single and combined OMW treatment (adapted from (Alver et al., 2015; Nieto et al., 2011b).	16
Table 2.4 Combined processes for OMW treatment (adapted from (Azabou et al., 2010; Lafi et al., 2009; Lucas et al., 2013)).	16
Table 2.5 Examples of main AOPs to treat OMW (adapted from (Lucas & Peres, 2009; Martins et al., 2010; Nieto et al., 2011a; Zazouli & Shahmoradi, 2019).	17
Table 2.6 Example of heterogeneous Fenton processes for treatment of OMW and simulated OMW (adapted from (Lucas & Peres, 2009; Martins et al., 2010; Nieto et al., 2011a; Zazouli & Shahmoradi, 2019).	21
Table 3.1 Composition of each synthetic solution used.	25
Table 3.2 Chemical structure and other proprieties for the used phenolic compounds.....	25
Table 3.3 Physicochemical characteristics of the OMW after 10-fold dilution.	26
Table A.1 H ₂ O ₂ concentration, absorbances and COD values at 620nm for the COD calibration curve.	55
Table A.2 Concentrations, mass, and dilution factor for each catalyst series and the correspondent iron weight in mass percentage.	57
Table A.3 Iron weight, mass, concentration, and iron leached in each catalyst.	57
Table C.1 TPh, TOC, COD removals, and H ₂ O ₂ consumption for real OMW using (a) 0.5 g L ⁻¹ , (b) 1.0 g L ⁻¹ , (c) 1.5 g L ⁻¹ of catalyst with [H ₂ O ₂] = 0.5 g L ⁻¹	61
Table C.2 TPh, TOC, COD removals, and H ₂ O ₂ consumption for real OMW at (a) T = 25 °C, (b) T = 50 °C and (c) T = 75 °C using [CAT] = 0.5 g L ⁻¹ and [H ₂ O ₂] = 0.5 g L ⁻¹	62

Notation and Glossary

BOD ₅	Biochemical Oxygen Demand	mg O ₂ L ⁻¹
C	Concentration	mg L ⁻¹
C ₀	Initial concentration	mg L ⁻¹
COD	Chemical Oxygen Demand	mg O ₂ L ⁻¹
d _p	Particle diameter	mm
H ₂ O ₂	Hydrogen Peroxide	mg L ⁻¹
TOC	Total Organic Carbon	mg C L ⁻¹
TPh	Total phenolic content	mg GA _{eq} L ⁻¹
V	Volume	L
X	Conversion/Removal/Consumption	%
wt.	Iron weight percentage	%

Greek Letters

λ	Wavelength	nm
---	------------	----

Indexes

°C	Celsius degree
----	----------------

List of Acronyms

AC	Activated Carbon
AOP	Advanced Oxidation Process
APHA	American Public Health Association
AS	Active Sites
CWPO	Catalytic Wet Peroxide Oxidation
D	Dilution Factor
DAD	Diode Array Detector
EDG	Electron Donor Group
ELV	Emission Limit Values
GA	Gallic Acid
HPLC	High Performance Liquid Chromatography
OMW	Olive Mill Wastewater
OS	Olive Stone
OSAC	Olive Stone-Activated Carbon

OSAC-Fe	Olive Stone-Activated Carbon-Fe
RMV	Recommendable Maximum Value
SEM	Scanning Electron Microscopy

1 Introduction

1.1 Framing and Presentation of the work

Fresh/potable water is a vital natural resource that is continuously threatened by the fast urbanization, intensified industrialization, and increasing climate changes at a global scale. Industrial residues, and particularly those generated by food processing industries, are the main source of environmental problems related to depletion of natural resources, soil erosion, air pollution and water contamination. To prevent such environmental threats and to secure the sustainability of natural and urban water cycles for future generations, the continuous research and development of innovative solutions for wastewater management is of crucial importance (Domingues et al., 2018; Fragoso & Duarte, 2012).

Olive oil production is a traditional agriculture activity with a great economic importance, the annual world production being estimated as approximately 3207 tonnes. The world's larger producers are situated in the Mediterranean Region: Spain, Italy, Greece, and Portugal, with ca. 1125, 366, 275, and 141 tonnes produced in the last year, respectively (Espadas-Aldana et al., 2019; International Olive Oil Council, 2018a, 2018b). Despite the economic and health benefits of olive oil production and consumption, olive oil extraction typically entails some environmental problems related to the properties and amount of the wastewaters generated, commonly known as olive mill wastewater (OMW) (Espadas-Aldana et al., 2019).

The physicochemical composition of OMW is highly variable depending, among others, on climate, type of olive, cultivation practice, and extraction process adopted. Generally, OMW presents a strong odor, dark red-brown color, slightly acidic pH, and an elevated organic load (composed mainly of polyphenols, like tannins, polyalcohols, pectins and lipids), which are phytotoxic due to the high phenolic content (Domingues et al., 2018). The high organic load is typically traduced in chemical oxygen demand (COD) values ranging between 45 - 180 g O₂ L⁻¹, biochemical oxygen demand (BOD₅) of 25 - 100 g L⁻¹, total phenol contents (TPh) of 2 - 15 g L⁻¹, total suspended solids (TSS) values of 24 - 120 g L⁻¹, mineral solids up to 15 g L⁻¹, and oils and fat ranging 0.5 - 1.0 g L⁻¹ (Domingues et al., 2019).

As a mean to handle OMW, some traditional physicochemical methods are used to initiate the effluent treatment, where the main goal is to remove the phenolic load, COD and increase biodegradability for further biological degradation. According to Domingues et al. (2019), filtration, coagulation, and flocculation processes only act in part of the problem, since they only operate in phase change, leading to the transfer of the organic pollutants into another phase, not destroying the organic compounds.

Advanced oxidation processes (AOPs) are one of the most promising and widely studied technologies used to eliminate the high organic load present in industrial wastewaters. AOPs are able to oxidize toxic pollutants into nontoxic biodegradable substances due to the formation of highly oxidative radicals, namely, hydroxyl radicals (HO^\bullet) (Sani et al., 2020).

Among several AOPs, the Fenton process stands out due to its ability to easily decompose organic contaminants at soft operational conditions (room temperature, atmospheric pressure, and overall low energy requirements) (Domingues et al., 2021). Despite the advantages, the classic Fenton process is operated in the homogenous phase which entails some disadvantages, such as the downstream formation of ferric sludge as a result of the high concentration of iron ions commonly required, and the dependence of an acidic pH medium to efficiently catalyze the reaction. To overcome these disadvantages, the use of solid catalysts is a possible solution since the sludge generation problem is overcome, and the reuse and recycling of the catalyst enables a reduction of operation costs (Domingues et al., 2018, 2019).

In the present work it is assessed the use of the heterogeneous Fenton process to treat OMW provided by an olive oil industrial unit, using a series of iron-supported catalysts prepared from a by-product of the same industry: olive stones (OS). For this purpose, synthetic phenolic mixtures simulating the polyphenolic composition in real OMW were selected. The adsorptive and catalytic activities of the different catalysts were evaluated in batch experiments, and some operational parameters were optimized, namely, catalyst particle size and catalyst load. Different initial compositions of the effluent were also studied. Afterwards, the most suitable catalyst under the optimized parameters was selected for the treatment of real OMW. In order to evaluate the process' performance, TOC (total organic carbon, as solution's mineralization degree indicator), COD and TPh removals, as well as H_2O_2 consumptions, were followed during the process, whereas the Fe leached from the support was also measured after each experiment to infer on the material's stability.

1.2 Contribution of the author

In the current work it is proposed the use of heterogeneous catalysts derived from olive residues in order to improve the treatment of olive oil discharges (solid and liquid). The main purpose of this work is to assure the maximum degradation of phenolic compounds using the selected catalysts, guarantee high performance and stability of the catalysts during the heterogeneous Fenton-like process, and assure an appropriate effluent treatment.

1.3 Organization of the thesis

In chapter 1 it is made a brief introduction about the olive oil industry, some general characteristics of the generated effluents and their environmental impacts. Some processes used to treat the discharged effluents are also addressed, and finally it is mentioned the main contribution of the author to the developed work.

In chapter 2 it is presented the state-of-the-art where it is provided, in detail, some important information about the hazardous contaminants of OMW and the most adequate processes/schemes for their treatment. Particularly, it is discussed the proposed catalytic treatment in this thesis - the heterogeneous Fenton process - and also the influence of some operating conditions of the oxidation reaction.

Chapter 3 mentions the main methods and materials applied in the experimental work, being detailed the preparation of the catalysts, the synthetic solutions used, as well as the adopted conditions during the experiments. The analytical methods applied for wastewater's characterization are also described.

Along chapter 4, the main results are analyzed and discussed taking into consideration the influence of the physical-chemical properties of the catalyst, along with the hydrogen peroxide dose, catalyst concentration, effluent's composition, and the effect of the reaction's temperature.

In chapter 5 are summarized the achieved goals, the encountered drawbacks during the developed work and the possible improvements for future work.

2 Context and State-of-the-art

Olive oil can be obtained by 3 major processes: traditional discontinuous press process, the 2-phase centrifugal process, and the 3-phase centrifugal process. The first process is the most traditional one; however, it offers a lower production yield of olive oil and higher labor costs. A scheme for 2-phase and 3-phase separation processes is shown in figure 2.1; they are continuous processes, and the best choice to produce olive oil at industrial scale. In the 3-phase separation process, larger amounts of water are required during olive oil extraction due to the continuous washing of the olive paste, approximately 6 m³/ton of olive oil, resulting in three streams at the decanter's exit: olive oil, pomace, and wastewater. On the other hand, the more recent 2-phase separation process eliminates almost completely the need of water in the extraction process, and therefore originates semisolid residues at the decanter's exit, together with the olive oil. Such residues are commonly called wet pomaces, with approximately 60 % of moisture, and can be further processed as to recover a lower-quality olive oil (called OOEIW - olive oil extraction industry wastewater). For this reason, nowadays most olive oil producing countries are updating their facilities to the 2-phase process (Amor et al., 2019; Domingues et al., 2021).

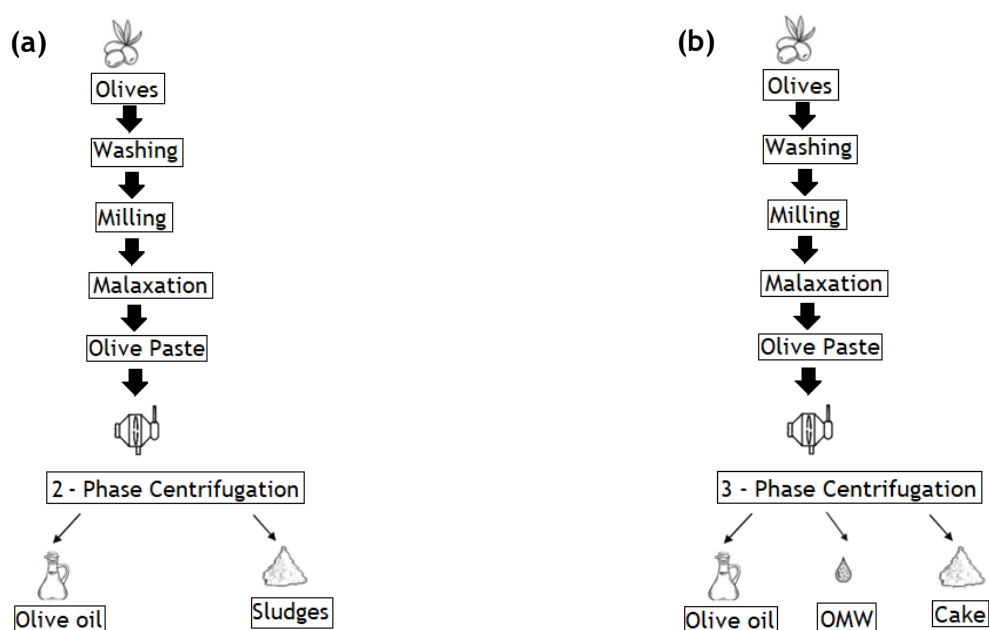


Figure 2.1 Overall scheme of the processes used for olive oil extraction: (a) 2-phase and (b) 3-phase centrifugation (adapted from Amor, C. et al., *Water*, 11 (2019) 5-29; Domingues, E. et al., *Journal of Water Process Engineering*, 39 (2021), 8).

Regardless of some improvements in the olive oil production, such as lower water demands, solid/liquid extraction processes for pomace oil recovery, and recycling of the solid wastes (e.g., burning for energy recovery), olive oil production still entails environmental and ecological problems. An important strategy to deal with the environmental impact of agriculture wastewaters consists in analyzing and assessing the main problems of the olive oil production using Life Cycle Assessment (LCA) tools (Espadas-Aldana et al., 2019). Extraction of the olive oil cake, generation of thermal/electrical energy, the re-use of water and nutrients for feeding livestock, the extraction of high added value by-products and production of biofuels, are some examples of valorization techniques used to develop a green and circular economy (Sánchez-Sánchez et al., 2020).

Another way of diminished the environmental impacts is the reuse of solid residues, as solid supports, in the heterogeneous Fenton process. These materials can be prepared, activated and finally impregnated with metals ions, such as iron, to oxidize organic compounds in wastewater treatment. Esteves et al.(2020) employed carbon supports derived from olive oil residues and it is an example of a sustainable and greener process to treat OMW, where oxidation of 50 - 56 % of phenolic content, and an improve of stability (low Fe leaching) and enhanced mineralization were achieved.

2.1 OMW's pollutants and environmental impacts of olive oil effluents

Despite its economic advantages, the olive oil industry has been associated with environmental issues related to depletion of natural resources, land degradation, and waste production. Worldwide, during the months of November till February, the production of olive oil originates a high amount of OMW and pomace by-products from the extraction process, as olive oil only represents ca. 20 % of the overall input volume (Babić et al., 2019).

The pollution potential of the OMW is typically associated with its high phenolic content, BOD and COD, high organic and solid matter content, presence of metals and mineral substances, such as potassium, phosphorus, and calcium. Generally speaking, OMW are very complex and heterogeneous effluents since their physical-chemical compositions are dependent on different factors such as the olive variety, olive cultivation, climate, and extraction process employed (Domingues et al., 2021). Table 2.1 highlights the main physico-chemical properties of OMW according to the extraction process.

Table 2.1 Physico-chemical properties of OMW using different processes (adapted from (Babić et al., 2019; Domingues et al., 2021; Nieto et al., 2011a).

Process	pH	Chemical Oxygen Demand (COD)	Biological Oxygen Demand (BOD ₅)	Total Suspended Solids (TSS)	Total Phenols (TPh)	Total Organic Carbon (TOC)
Traditional (Babić et al., 2019)	4.4	130 (g L ⁻¹)	41 (g L ⁻¹)	26 (g L ⁻¹)	9 (g L ⁻¹)	44 (g L ⁻¹)
3-phase (Domingues et al., 2021)	4.8	50 (g L ⁻¹)	8 (g L ⁻¹)	0.6 (g L ⁻¹)	4 (g L ⁻¹)	-
2-phase (Nieto et al., 2011a)	6.3 - 7.2	1673 - 4137 (mg O ₂ dm ⁻³)	380 - 1100 (mg O ₂ dm ⁻³)	0.001 - 0.005 (% w/w)	44 - 51 (mg O ₂ dm ⁻³)	-

Usually, the amount of phenolic compounds present in OMW depends on the olive fruit and their maturity, climatic conditions, processing, and storage. There are 3 main families of phenolic compounds, the cinnamic acids, benzoic acids and tyrosol derivatives responsible for the high toxicity of these effluents. The negative impacts of these compounds are caused mainly due to the auto-oxidation into reactive oxygen species, such as, superoxides, and the interference in the respiratory chain and the mitochondrial phosphorylation system. The previous effects also impacts toxicity into aquatic and soil microorganisms, invertebrates, crop plants and soils, leakage in underground aquifers, pollution of water bodies, and inhibition of auto purification processes, highlighting the problematic of the untreated OMW and the proper treatments for these effluents (Justino et al., 2012; Ochando-Pulido et al., 2017).

Among the available EU directives, the concern about dangerous and hazardous substances began with the introduction of the directive 76/464/EEC (The Council of the European Communities, 1976) and renamed as 2006/11/EC (Commission, 2006). This directive legislates the levels of each dangerous substance into the aquatic environment. In Portugal, the physico-chemical parameters of the water quality are fixed according to the Decree-Law no. 236/98 (table 2.2).

Table 2.2 Physico-chemical parameters for water consumption with Recommendable values (VMR) in Portugal and Emission Limit Values (ELV) of residual waters in Porto (adapted from (Diário da República, 1998; SIMDOURO-Grupo Águas de Portugal, n.d.)).

Parameters	(Diário da República, 1998) (VMR)	(SIMDOURO-Grupo Águas de Portugal, n.d.) (ELV)
pH	6.5-8.5	5.5-9.5
Temperature	12 °C	30 °C
BOD ₅	-	500 mg O ₂ L ⁻¹
COD	-	1000 mg O ₂ L ⁻¹
Phenols	0.5 µg L ⁻¹ C ₆ H ₅ OH	1 mg L ⁻¹ C ₆ H ₅ OH
Total Iron	50 µg _{Fe} L ⁻¹	2.5 mg _{Fe} L ⁻¹

Comparing the values from tables 2.1 and 2.2, it can be said that industrial OMW presents in its' constitution 100 times higher values of COD, and 50 - 5000 times higher values of phenols in comparison with those legislated, which means that it is necessary to apply strategies to guarantee the quality of the treated water and prevent any risk of environmental impact. Among these strategies are the use of physico-chemical treatments and oxidation processes to remove BOD and TSS, up to 85 %, whereas reducing ammonia, phosphorous, and nitrogen concentrations over 50 % (Domingues et al., 2021).

2.2 Physical-chemical processes for OMW treatment

OMW are typically composed by high concentration of suspended solids, resulting from the olive fruit, and also dissolved organic matter in high concentration, as seen before, which implies the use of physico-chemical procedures, such as coagulation-flocculation and AOPs, to handle the OMW treatment (Ochando-Pulido et al., 2017). Coagulation-flocculation process is one of the most common wastewater treatments were some compounds, such as aluminum sulfate ($\text{Al}_2(\text{SO}_4)_3 \cdot 16\text{H}_2\text{O}$), aluminum chloride (AlCl_3), ferric chloride ($\text{FeCl}_3 \cdot 6\text{H}_2\text{O}$), and/or other polymers are added to the effluent to create large flocs from the particles present in OMW. Some examples of OMW treatment based on coagulation and flocculation are presented in table 2.3.

Table 2.3 Coagulation-flocculation processes as single and combined OMW treatment (adapted from (Alver et al., 2015; Nieto et al., 2011b)).

Authors	Process	Conditions	Results
(Nieto et al., 2011b)	Flocculation-sedimentation using commercial flocculants and oxidation processes	[Coagulant] = 0.05 mg dm ⁻³	COD: 661 mg O ₂ L ⁻¹ Fe removal: 99.5 % and 99.6 % Total phenols: 0.005 mg dm ⁻³
(Alver et al., 2015)	Coagulation and Fenton using FeSO ₄ .7H ₂ O as coagulant and catalyst	[Fe ²⁺] = 2.5 g L ⁻¹	COD removal of 58.4 % TOC removal of 47.8 % TPh removal of 77.2 % BOD ₅ /COD ratio of 0.2259

Despite the previous results, coagulation-flocculation, and other processes still present some limitations in eliminating some organic matter, phenolic compounds and the respective intermediates. In order to minimize these limitations, some strategies consider the combination of biological treatment processes with other processes to decrease the non-biodegradable components (Lafi et al., 2009). One example of the importance of the biological processes is demonstrated in Amor et al. (2015) work combining the Fenton process with anaerobic process using microorganisms to treat OMW and improve the biodegradability. First it was obtained COD reductions of 17.6 % and 82.5 % of TP, after the biological treatment it was obtained COD reductions from 64 % to 88 % proving that AOP and biological processes are effective in OMW treatment, other examples being presented in table 2.4.

Table 2.4 Combined processes for OMW treatment (adapted from (Azabou et al., 2010; Lucas et al., 2013)).

Authors	Process	Conditions	Results
(Azabou et al., 2010)	Combination of WHPCO process and anaerobic digestion	[Phenol] ₀ = 1.25 g L ⁻¹ [Catalyst] = 0.5 g L ⁻¹ [H ₂ O ₂] = 2 × 10 ⁻² M T = 25 °C	COD reduction = 37 % Phenol reduction = 54 %
(Lucas et al., 2013)	Fenton's Reagent pretreatment combined with aerobic process	H ₂ O ₂ /COD ratio = 0.20 H ₂ O ₂ /Fe ²⁺ = 15 [COD] ₀ = 92.5 g L ⁻¹	COD removal = 81 % TPh removal = 94 %

(a) ozonation + aerobic digestion; (b) UV + aerobic digestion

AOPs are promising technologies for the degradation of resistant and recalcitrant compounds leading to their partial degradation or partial mineralization. In these processes, highly oxidizing species are produced, like hydroxyl radicals (HO^\bullet), which are characterized by the high oxidation potential and the non-selective nature that allows the decomposition of organic contaminants into CO_2 , H_2O , and inorganic ions (Márquez et al., 2018). AOPs include ozonation, Fenton's process, photocatalysis, electrochemical processes, hybrid processes, among others (Ochando-Pulido et al., 2017). Some examples of AOPs used to treat OMW are shown in table 2.5.

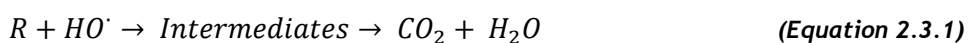
Table 2.5 Examples of main AOPs to treat OMW (adapted from (Lucas & Peres, 2009; Martins et al., 2010; Nieto et al., 2011a; Zazouli & Shahmoradi, 2019).

Authors	Process	Results
(Martins et al., 2010)	Heterogeneous Fenton process with ceria-based catalysts	TPh removal = 100 % TOC removal = 57 %
(Zazouli & Shahmoradi, 2019)	Homogenous Fenton process for OMW treatment	COD removal = 82 % BOD removal = 60 % TOC removal = 57 %
(Lucas & Peres, 2009)	Homogenous Fenton process using $\text{FeSO}_4 \cdot 7\text{H}_2\text{O}$ as catalyst	COD removal = 70 %
(Nieto et al., 2011a)	Homogenous Fenton process using FeCl_3 as catalyst	COD and phenolic compounds removals > 95 %

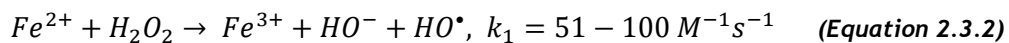
2.3 The Fenton process

The Fenton reagent involves the catalytic decomposition of hydrogen peroxide (H_2O_2) using an iron salt (Fe^{2+}), in acidic medium, to form hydroxyl radicals (HO^\bullet), a strong oxidizing agent capable of transforming pollutants into harmless subproducts such as CO_2 , H_2O , and inorganic salts (equation 2.3.1) (Sani et al., 2020).

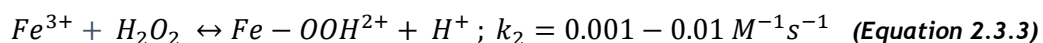
The Fenton's process provides many operational advantages as it may be conducted at atmospheric pressure and room temperature, and in the absence of almost any energy consumption (Neyens & Baeyens, 2003).



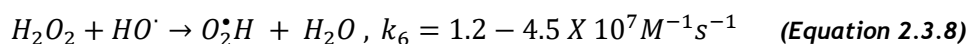
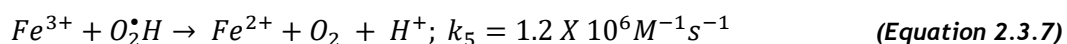
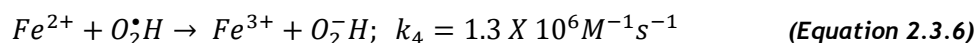
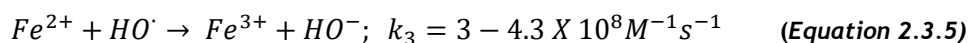
The mechanism proposed to explain the Fenton process is the Haber-Weiss mechanism, where the active species (HO^\bullet) are generated to degrade the organic compounds (Xu et al., 2020). The overall mechanism is given by the following general equation (equation 2.3.2) (Gil et al., 2010).



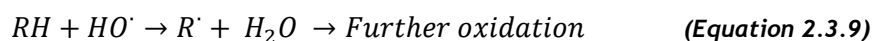
Since Fe^{2+} is the catalyst, it is necessary to be reestablished, this is possible thanks to regenerative reactions, such as those shown in equations 2.3.3 and 2.3.4 (Gil et al., 2010).



The generation of HO^\bullet and $^\bullet OOH$ (hydroperoxyl radical, less oxidizing than the hydroxyl radical) can be described through a series of complex reactions, as shown in equations 2.3.5 to 2.3.8 (Gil et al., 2010).



In some cases, iron species and H_2O_2 , cf. equations 2.3.5 and 2.3.8, can consume HO^\bullet radicals resulting in a scavenging effect and decrease the amount of available radicals for degradation (Gil et al., 2010). When the scavenging effect is minimum or absent, the HO^\bullet radicals oxidize the organic compounds (RH) due to the removal of protons originating organic radicals (R^\bullet). These are highly reactive and proceed to further oxidation, cf. equation 2.3.9 (Gil et al., 2010).



2.4 Parameters of influence on the Fenton's process

In order to optimize the Fenton process, there are some operation parameters that can improve the overall performance. The most important ones are the reaction's temperature, pH, concentration of H_2O_2 , catalyst load, and initial organic load of the solution/effluent to treat.

2.4.1 pH

The performance of the Fenton's reaction is highly reliant on pH levels, if pH values are lower than the optimum value the reaction between Fe^{3+} and H_2O_2 is inhibited due to the formation of intermediates (peroxocomplexes), cf. equations 2.3.6 and 2.3.7, contributing to a decreased performance. On the other hand, if the pH remains between $3 < pH < 4$, the previous intermediates are soluble and the H_2O_2 degradation is favored cf. equation 2.3.8 (Gil et al., 2010). On the other hand, high pH values ($pH > 4$) enables hydrolysis and precipitation of iron species (equation 2.3.7), decreasing the amount of catalyst available for the process. In addition, stability of the oxidant (H_2O_2) is detrimentally affected at high pH values (Gil et al., 2010; M. hui Zhang et al., 2019).

Tatibouët et al. (2005) studied the effect of pH on the homogenous and heterogeneous Fenton's reactions using pH values 2-4.5. It was concluded that both systems are very dependent on pH values, and the optimal pH is 3.7 since HO^\bullet production was maximum. Also Hodaifa et al. (2013) worked on the optimization of Fenton's reaction for OMW treatment by studying the pH effect on OMW degradation. It was attained maximum COD removal (72 %) at $pH = 3$ while at $pH = 7$ the removal efficiency decreased to 67 %, operating near room temperatures, $[H_2O_2] = 20 \text{ g dm}^{-3}$, and $[Fe^{3+}] = 0.04 \text{ g dm}^{-3}$.

2.4.2 Temperature

Another important factor is the temperature due to the increase in the reaction rate. According to Arrhenius law, equation 2.4.1, the rate constant (k_0) increases exponentially with temperature (Duarte, 2013).

$$k = k_0 e^{\left(\frac{E_a}{RT}\right)} \quad (\text{Equation 2.4.1})$$

Despite the increase of temperature favors the degradation rate, usually temperatures higher than $70 \text{ }^\circ\text{C}$ are not advisable in the Fenton's process since it contributes to H_2O_2 thermal decomposition into oxygen and water, equation 2.4.2 (Duarte, 2013).



Nieto et al. (2011a) studied the effect of the temperature during homogenous Fenton -like reaction performing two tests using temperatures of 278, 283, 288, and 293 K as near room temperatures and 303 K, and 313 K as high temperatures, maintaining $[H_2O_2] = 45 \text{ g dm}^{-3}$, $[Fe^{3+}] = 4.0 \text{ g dm}^{-3}$ and $pH = 3$. COD removals between 77 % to 89 % and total phenols removal of 99 % were maintained in all range of temperatures, the COD degradation increasing with the temperature; however, at 303 K, thermal degradation of H_2O_2 prevails more than organic degradation.

2.4.3 H_2O_2 concentration

In Fenton's reaction the presence of parallel reactions, cf. equation 2.3.8, and H_2O_2 decomposition, cf. equation 2.4.2, leads to a HO^\bullet consumption. Thus, to guarantee a full oxidation, it is necessary to apply an stoichiometric surplus of oxidant reagent (Duarte, 2013). Although the increase of oxidant leads to an increase of HO^\bullet production, and therefore an increase of organic degradation, the surplus needs to be carefully calculated in order to avoid an increase of HO^\bullet scavenging and production of $^\bullet OOH$, resulting in a significant decrease of the reaction's performance and also contributing to an wastage of oxidant and expenses (Duarte, 2013).

Domingues et al. (2021) studied the impact of H_2O_2 concentration during the OMW treatment using coagulation and the Fenton's process to treat OMW using different concentrations of H_2O_2 and $[Fe^{2+}] = 2 \text{ g L}^{-1}$, $pH = 3$ during 60 min. The authors concluded that using load of 28 g L^{-1} and 4 g L^{-1} of H_2O_2 lead to COD removals of 53 % and 30 % respectively.

2.4.4 Catalyst load

The most important parameter to optimize is the catalyst load since Fe^{2+} catalyzes the decomposition of H_2O_2 to produce highly oxidative HO^\bullet radicals. The increase of Fe^{2+} enhances the H_2O_2 decomposition and the production of HO^\bullet radicals, subsequently increasing the organic decomposition; however, an excessive amount of Fe^{2+} might increase the HO^\bullet scavenging effect, cf. equation 2.3.5 (Queirós, 2014).

Hodaifa et al. (2013) studied the consumption of H_2O_2 with and without Fe^{2+} . The authors noticed a COD removal of 67 % and phenolic compounds removal of 99 % in the absence of the catalyst, whereas the use of catalyst ($[Fe^{2+}] = 0.04 \text{ g dm}^{-3}$) led to an increase of COD removal reaching 74 %, which means that the presence of Fe^{2+} enabled the decomposition of H_2O_2 .

Domingues et al. (2021) also studied the effect of the iron catalyst load by performing a series of experiments using iron concentrations between $0.1 - 3.0 \text{ g L}^{-1}$, and $[H_2O_2] = 4 \text{ g L}^{-1}$ at $pH = 3$. The authors observed that when using 2.5 g L^{-1} of catalyst, the maximum COD removal (40 %) was reached, while using a concentration of 3.0 g L^{-1} , the COD removals decreased. This observation was explained by the scavenging effect of HO^\bullet resulting from the excess of catalyst load.

2.5 Heterogeneous Fenton process or Fenton-like reactions

The homogeneous Fenton process presents a series of associated disadvantages, the main drawback being the excessive use of iron which causes the formation of ferric sludge, where it is necessary to increase pH levels to promote iron precipitation and removal. Other drawbacks are formation of high concentration of ions and dependence of the H_2O_2 concentration levels (Domingues et al., 2019).

As a mean to overcome these handicaps, new approaches to the traditional Fenton reaction have been studied in the last years. One of the most promising approaches is the replacement of aqueous Fe^{2+} ions by a solid catalyst containing iron in its constitution, the so-called heterogeneous Fenton reaction, or catalytic wet peroxide oxidation (CWPO). The use of the heterogeneous Fenton presents some benefits like minimal leach of iron into the solution, and thus the minimal production of iron sludge, high catalytic activity, long term stability, easy catalyst recovery and high efficiency at broader ranges of pH values (Sani et al., 2020).

Martins et al. (2010) used a Fenton-like process with Fe-Ce-O catalyst, $[\text{H}_2\text{O}_2] = 224 \text{ mM}$, $[\text{Fe-Ce-O}] = 1.0 \text{ g L}^{-1}$ and $\text{pH} = 3.0$ to treat phenolic wastewaters and obtained a complete phenolic degradation and a TOC removal of 57 % after 120 min of reaction. Other studies using heterogeneous Fenton process are displayed in table 2.6.

Table 2.6 Example of heterogeneous Fenton processes for treatment of OMW and simulated OMW (adapted from (Esteves et al., 2020; Maduna et al., 2018).

Authors	Process	Conditions	Results
(Esteves et al., 2020)	Heterogeneous Fenton-like for treatment of simulated OMW	$[\text{H}_2\text{O}_2] = 1.0 \text{ g L}^{-1}$ $[\text{Catalyst}] = 0.5 \text{ g L}^{-1}$ $T = 25 \text{ }^\circ\text{C}$ $\text{pH} = \text{unadjusted}$	TPh removals = 50-56 % H_2O_2 consumption = 58 %
(Maduna et al., 2018)	CWPO of phenolic compounds in OMW using Cu catalysts	$[\text{Catalyst}] = 0.5 \text{ M}$ $m_{\text{Catalyst}} = 2.5 \text{ g}$ $T = 353\text{K}$	Complete TPh degradation TOC removals = 52 %

2.6 Activated carbons as catalysts in the heterogenous Fenton process

Activated carbons (ACs) in heterogeneous catalysis are popular solid catalysts/supports due to their unique properties that provide important advantages. The most important one is the presence of a large surface area and well-developed porosity, which originates a good dispersion of the active phase and increases resistance when operating at elevated temperatures under reaction (Barroso-Bogeat et al., 2020). These advantages are provided from the activation step where the presence of gases allows the development of the porous structures originating an elevated specific surface area that may reach about $1200 \text{ m}^2 \text{ g}^{-1}$, as well as high amount of micropores enabling the support of metal ions (Figueiredo & Ramôa Ribeiro, 2015).

In figure 2.2, scanning electron micrographs of an AC material are shown. It can be seen an irregular structure with plenty of cracks and fissures but also some smooth open pores that resulted from the activation process and other thermal treatments. Usually in activated carbons, the larger pores at the surface are connected to other smaller pores, meso or micropores, that are found inside of the carbon material. It is also visible some brighter spots and other irregular small structures that are a result of inorganic compounds that come naturally in the mineral structure or result from the activating agent during the preparation/treatment processes or even products of surface reactions (Barroso-Bogeat et al., 2020).

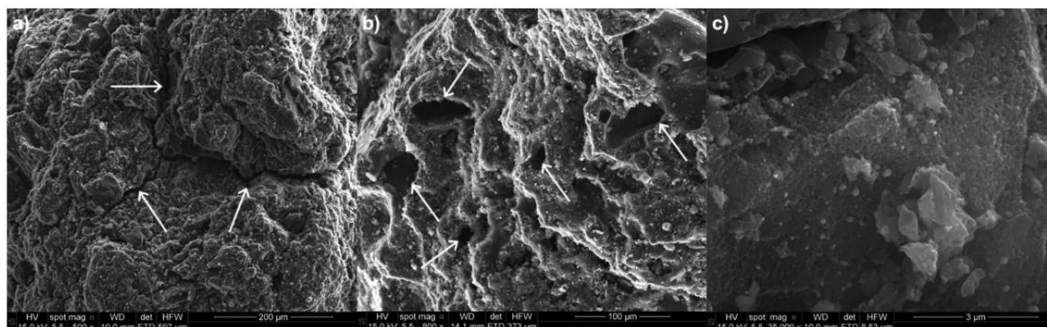


Figure 2.2 SEM images of an AC surface at different magnifications, the scale corresponding to the reference lengths: (a) $200 \mu\text{m}$, (b) $100 \mu\text{m}$, and (c) $3 \mu\text{m}$ (adapted from Barroso-Bogeat et al. 2020)

The presence of oxygen groups in the activated carbon surface can improve the dispersion of the active phase in the catalyst since they provide sites or nucleation centers during the adsorption and impregnation processes. The presence of carboxylic acids, phenols, and carbonyls decrease the hydrophobic character of the AC improving the solution-catalyst contact. Gas/liquid oxidation treatments can be implemented to introduce these oxygen functionalities in the catalyst surface (Barroso-Bogeat et al., 2020; Pinho et al., 2020).

Another important advantage of ACs is the presence of reduced active sites (AS), i.e. electron donor sites, and oxidized active sites (AS⁺) originating strong and unstable active species reacting with different compounds, namely, H₂O₂, making the ACs suitable supports for CWPO reactions (Pinho et al., 2020)

Some metal-based impurities in ACs can also present some catalytic activity (Navalon et al., 2011). Pinho et al. (2020) studied the role of different parameters, including the presence of iron impurities in ACs, and concluded that higher iron impurities resulted in better performances in CWPO. To confirm the importance of impurities, the authors determined the iron leached into the solution and confirmed that the higher iron leached values belong to the higher iron content catalysts.

Other advantages presented by ACs are the resistance to heat and radiation, good mechanical strength and stability when in contact with acid/basic solutions, and the lowest cost when compared with other catalysts (Pinho et al., 2020).

3 Materials and Methods

3.1 Catalysts preparation

The catalysts used in this study were developed using the same method and conditions employed in the work developed by Esteves et al. (2020). Olive stones (OS) were rinsed, grinded, and sieved to obtain particles with three size fractions: $0.80 < d_p < 1.0$, $0.45 < d_p < 0.80$, and $d_p > 0.25$ mm. Then, the different OS fractions were carbonized in a horizontal tube furnace for 2 hours at 800 °C in the presence of an inert gas (N₂), to produce OS-biochars. Following this step, physical activation of the samples was performed using CO₂. For that, the N₂ stream was replaced by CO₂ for 4 hours (at 800 °C). After the activation process, the flow of CO₂ was turned off and samples were allowed to cool to room temperature under a nitrogen flux. After the activation process, the flow of CO₂ was turned off and samples were allowed to cool to room temperature under a nitrogen flux.

Afterwards, the produced olive stone activated carbon (OSAC) support was impregnated with Fe to obtain a theoretical load of 5 wt.% employing the incipient wetness impregnation method (IWI), or capillary impregnation, using Fe(NO₃)₃·9H₂O MSDS (Merckmillipore) as iron-precursor. In this method, the metal precursor is dissolved in the minimum amount possible of distilled water, then this solution is dropped over a layer of the catalyst to fill the OSAC pores. In order to obtain the real amount of iron in the OSAC catalyst, it was calculated the iron weight percentage (wt(%)). Then, the catalyst is dried at 100 °C overnight, to eliminate volatile organic compounds, and in the end, the catalyst was thermally treated at 350 °C with N₂ for 1 hour, cooled down and sealed.

3.2 Synthetic and real OMW composition and experimental procedure

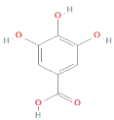
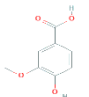
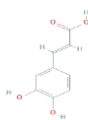
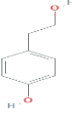
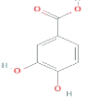
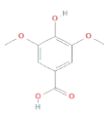
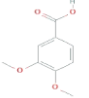
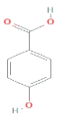
For the laboratorial experiments, both synthetic solutions and real OMW samples were used. Due to the heterogeneous and variable composition of real OMW samples, screening of the materials was first performed with synthetic polyphenolic solutions. To prepare the synthetic solutions, different phenolic compounds commonly present in real OMW were used to obtain solutions with different but well-controlled compositions. The concentration of each compound was calculated to obtain a solution with a TPh concentration of 350 mg L⁻¹. All compounds were dissolved in distilled water, homogenized with an ultrasonic bath to ensure full dissolution, and preserved in the dark and dry place at room temperature. Throughout the tests, three synthetic solutions were evaluated with different phenolic compositions, as shown in table 3.1. In table 3.2 it is presented the chemical structure and other properties of the selected phenolic compounds.

Table 3.1 Composition of each synthetic solution used.

	CA	VA	GA	TY	PA	SY	VER	4-HYD.
SYNTHETIC-1	X	X	X	X	X	-	-	-
SYNTHETIC-2	X	X	X	-	-	X	X	-
SYNTHETIC-3	X	-	-	X	-	X	X	X

CA - Caffeic acid; VA - Vanillic acid; GA - Gallic acid; TY - Tyrosol; PA - Protocatechuic acid; SY - Syringic acid; VER - Veratric acid; 4-HYD - 4-Hydroxybenzoic acid.

Table 3.2 Chemical structure and other proprieties for the used phenolic compounds.

Name	Chemical Structure	Molecular Formula	Molecular weight (g mol ⁻¹)
3,4,5-Trihydroxybenzoic acid (Gallic Acid)		C ₇ H ₆ O ₅	170.12
3-Methoxy-4-hydroxybenzoic acid (Vanillic acid)		C ₈ H ₈ O ₄	168.15
3,4-Dihydroxycinnamic acid (Caffeic acid)		C ₉ H ₈ O ₄	180.16
2-(4-Hydroxyphenyl) ethanol (Tyrosol)		C ₈ H ₁₀ O ₂	138.16
3,4-Dihydroxybenzoic acid (Protocatechuic acid)		C ₇ H ₆ O ₄	154.12
4-Hydroxy-3,5-dimethoxybenzoic acid (Syringic acid)		C ₉ H ₁₀ O ₅	198.17
3,4-Dimethoxybenzoic acid (Veratric acid)		C ₉ H ₁₀ O ₄	182.17
4-Hydroxybenzoic acid		C ₇ H ₆ O ₃	138.12

The real OMW used in this study was obtained from a 3-phase olive oil extraction unit of an olive mill located in Barcelos, Portugal, in late 2019. Samples were collected directly from the extraction centrifuges, allowed to sediment with the aim to collect the supernatant, that was divided into 1 L containers and frozen until needed. Prior to the catalytic experiments, the solution was diluted 10-fold as to simulate OMW's conditions after collection from an open-air pond (i.e. after mixing with olives washing wastewater and subject to climate conditions such as dilution by rain). The principal physicochemical characteristics of the real OMW are displayed in table 3.3.

Table 3.3 Physicochemical characteristics of the OMW after 10-fold dilution.

Parameters	After Dilution (D=10X)
CQO (mg L ⁻¹)	1094 +/- 10
TOC (mg L ⁻¹)	527 +/- 5
TPh (mg L ⁻¹)	47.7 +/- 0.4
pH	3.4 +/- 0.1
T (°C)	23.7 +/- 0.3

The experiments were carried in a batch reactor with a volume of 370 mL, covered with silver foil to prevent the action of photodegradation. The reactor's jacket was connected to a thermostatic bath (VWR) to control the reaction temperature. A magnetic agitation at 300 rpm (AGIMATIC S, J.P.Selecta) and a pH-meter (EDGE pH-meter, HANNA Instruments) were also employed. The experiments started with an initial volume of 150 mL, with $T_0 = 25^\circ\text{C}$, $\text{pH} = 3.5 - 4.0$ (i.e., solution's unaltered initial pH). At the same time, the solid catalyst was weighted, accordingly to the chosen concentrations, and added to the reactor. It was set up a timer since the addition of the catalyst until the end of the reaction. During the experiments, several samples were collected over time. To properly evaluate the catalytic activity of the materials, all catalysts were previously saturated prior to the addition of the oxidant; for $[\text{CAT}] = 0.50 \text{ g L}^{-1}$ this was achieved under 180 min, and for $[\text{CAT}] = 2.5 \text{ g L}^{-1}$ the saturation was reached at 240 min.

Then, a certain amount of H_2O_2 (30% w/v, VWR Chemicals) was added to the reactor in order to start the oxidation process. The amount of H_2O_2 used in the reaction was calculated to be in stoichiometric excess to completely oxidize the phenolic compounds ($[\text{H}_2\text{O}_2] = 500 \text{ mg L}^{-1}$). Prior to analytical analysis, samples collected during the experiments were passed through 0.45 μm filters (GE Healthcare) to separate the catalyst from the solution. Different fractions of the filtrated solution were used to determine the phenolic compounds (by high-performance liquid chromatography - HPLC, as described below), the H_2O_2 concentration, and to measure the solution's TOC. TOC and TPh removals for the synthetic solutions were calculated using

equation 3.2.1. In the case of real OMW, the phenolic removal was obtained using the Folin-Ciocalteu method and the correspondent concentrations obtained using a calibration curve with GA as the standard and results reported as mg GA_{eq}/L. The COD values were measured using the 5220 COD method provided from APHA (American Public Health Association (APHA) et al., 1998). It was also calculated the amount of iron leached into the solution using atomic absorption spectroscopy (AAS).

$$X = \frac{c_0 - c}{c_0} * 100 \quad \text{Equation 3.2.1}$$

The iron weight percentage (wt.%) was also calculated. For the digestion, the catalyst is weighted and transferred to a digestion flask where are added 7 ml of HNO₃, 7 ml of deionized H₂O, and 1 ml of H₂O₂. In the end, the samples are put into a microwave digester for 45 min at 200 °C. After the digestion, AAS was employed to determine a specific dissolved metal (Fe³⁺) in a liquid sample using a flame to vaporize the sample and detect the free metallic atoms (Freedman, 2012) and then calculate the amount of iron leached into the solution.

3.3 Analytical techniques

As a mean to quantify the amount of the phenolic content present in the synthetic solution along the CWPO experiment, the HPLC apparatus (Hitachi) was used, equipped with a diode-array detector (DAD), consisting of an L-2310 pump, L-2200 auto-sampler, and L-2455 DAD. The separation was achieved using a STAR RP-18 (Purospher) column (240 mm x 4 mm, 5 µm) at 50 °C as standard oven temperature. It was adopted a mobile phase consisting in 70% (v/v) of ultra pure water, slightly acidified with 0.1% orthophosphoric acid (v/v), and 30% (v/v) of methanol (VWR Chemicals). In order to identify the compounds, each calibration curve was obtained individually, see appendix A.1. The injection volume used was 20 µL and spectra records were made at 280 nm.

The quantification of H₂O₂ was made by the colorimetric method developed elsewhere (Sellers, 1980), where the formation of a yellow-orange complex, resulting from the interaction between H₂O₂ and titanium IV, is detected at 400 nm using a spectrophotometer (Helios, Thermo Scientific). The concentration of H₂O₂ was obtained using the calibration curve presented in appendix A.2.

For the experiments where real OMW solutions were used, the total amount of phenolic compounds was obtained using the Folin-Ciocalteu reagent, where the phenolic compounds from the solution react with this reagent to form a blue complex quantified by spectroscopy (Hudz et al., 2019). After allowing the color to develop for 2 h in dark, the solution's absorbance was measured at 765 nm (Demiray et al., 2011). The phenolic concentration was determined using the calibration curve presented in appendix A.3.

The total organic content includes a variety of organic compounds in a diverse oxidation states, the total organic carbon (TOC) measures are a convenient and a direct expression of the total organic content, since these values are independent of the organic oxidation state and does not include other organic bound (American Public Health Association (APHA), 1999). TOC measurements were performed using a TC/TOC-L model apparatus from Shimadzu.

The organic and inorganic contaminants in solution subject to oxidation were measured following the 5220 COD method (American Public Health Association (APHA) et al., 1998). In this method it is used 3.5 ml of a standard sulfuric acid solution (500 ml H₂SO₄ and 5.0 g AgSO₄), 2.5 ml of sample and 1.5 ml of a standard dichromate solution (2.55 g K₂CrO₇; 41.8 ml H₂SO₄ and 7.33 g HgSO₄). Then, the tubes are placed into a digester at 150 °C for 2 hours and let it cool down at room temperature, lastly it is measured the absorbance using Nanocolor 500D, (Macherey-Nagel) at 620 nm. The COD calibration curve is presented in appendix A.4.

In order to obtain the wt. (%), it was performed an acid digestion and calculated the correspondent amount of iron using an AAS UNICAM spectrophotometer (939/959 model), values of 5.74 %, 4.25 % and 4.79 % of iron being obtained for $0.80 < d_p < 1.0$, $0.45 < d_p < 0.80$, and $d_p > 0.25$ mm, respectively. The iron leaching values are presented in table A.2, appendix A.5.

4 Results and discussion

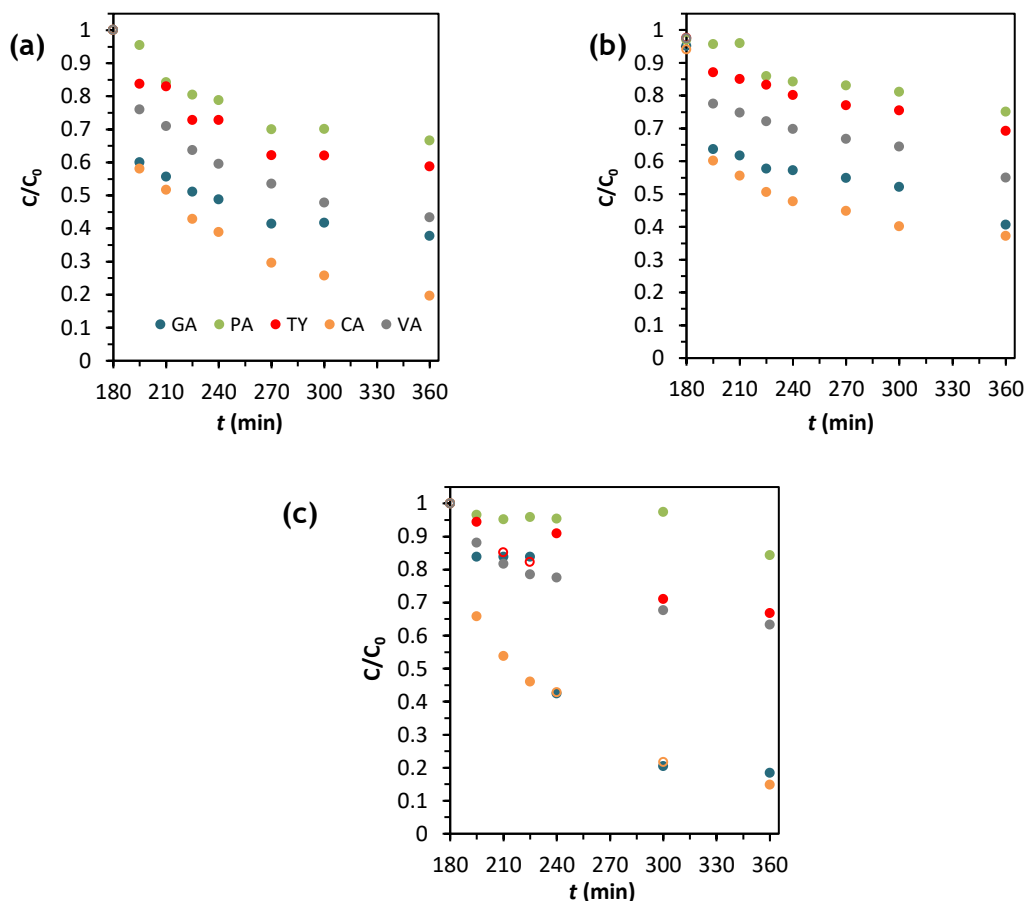
4.1.1 Influence of catalyst's particle size

The influence of the catalyst's particle size during the oxidation process was the first parameter to be studied in the degradation of the synthetic polyphenolic solution (SYNTHETIC-1, cf. table 3.1), using $[CAT] = 0.5 \text{ g L}^{-1}$, $[H_2O_2] = 0.5 \text{ g L}^{-1}$ at $T = 25 \text{ }^\circ\text{C}$ and unaltered solution's initial pH of 3.6. Due to the predicted adsorptive capacity of the synthesized activated carbon-based catalysts, the influence of the adsorption phenomena was evaluated prior to oxidation. Experiments were therefore conducted for 360 min, where the first 180 min corresponds only to the adsorption of phenolic compounds onto the OSAC-Fe catalysts.

The adsorption process is the first step of a catalytic reaction since there is a weakening of the chemical bonds and posterior chemical transformation, where first, the phenolic compounds are linked to the catalyst surface (Figueiredo & Ramôa Ribeiro, 2015). This process depends on the catalyst structure but also on the chemical interactions, nature, and chemical structure of the phenolic compounds. Overall, the adsorption of phenolic groups is promoted by electron withdrawing groups in the substituents but also their position (Esteves et al., 2020).

In appendix B.1 is presented the ratio C/C_0 during the adsorption process (180 min) for each catalyst, where C and C_0 represent the sum of all phenolic compounds in the solution at any time t and at $t = 0$, respectively. It is clear that the catalysts with bigger particle sizes present similar organic removals (ca. 4 % removal after 180 min) which were higher (ca. 12 %) for the one with the smallest particle size ($d_p < 0.25 \text{ mm}$). The presence of electron donor groups (EDG) in hydroxycinnamic acids, such as caffeic acid, enhances the bonds with iron-based catalysts due to the presence of ethylene group ($C=C$), which helps to explain the favorable removal of this compound by such materials (Esteves et al., 2020).

Regarding the catalytic oxidation, results in figure 4.1 (a) show, for case of the higher particle size, a higher removal of caffeic and gallic acids, reaching 80 % and 62 % at the end of the 360 min process time, respectively, and lower removals of tyrosol and protocatechuic acid (41 % and 33 %). According to Esteves et al. (2020), the oxidation of caffeic and gallic acids are favored due to the electrophilic attack of EDG. As stated before, the cinnamic derivatives are easier removed, however, the presence of 3-OH groups also facilitates the oxidation of gallic acid, over vanillic acid, since the electrophilic attack is enhanced. Trends are more or less the same for the other catalyst particle sizes (figure 4.1).



CA - Caffeic acid; VA - Vanillic acid; GA - Gallic acid; TY - Tyrosol; PA - Protocatechuic acid;

Figure 4.1 Removal of each phenolic compound (C/C_0) over time during the catalytic process using catalysts with different particle sizes (d_p) (a) $0.80 < d_p < 1.0$ mm, (b) $0.45 < d_p < 0.80$ mm, and (c) $d_p < 0.25$ mm. Experimental conditions: SYNTHETIC-1 solution, $[CAT] = 0.5 \text{ g L}^{-1}$, $[H_2O_2] = 0.5 \text{ g L}^{-1}$, $T = 25 \text{ }^\circ\text{C}$, and $pH = 3.6$.

An overview of the whole process is given in figure 4.2, where it is possible to analyze the concentration of all phenolic compounds over time for both adsorption and catalysis, for the three different particle size ranges. In figure 4.2 it is clear a stabilization of C/C_0 values during the initial minutes, corresponding to the adsorption process, ca. 4-12 %. After 120 min the catalyst surface starts to be saturated, reaching the saturation at 180 min; afterwards, the oxidizing reagent (H_2O_2) is added and the oxidation begins, resulting in a clearly decrease on the phenolic compounds concentration values. A slightly better performance using the bigger particle size catalyst is noticeable, but at the end of the process performances are not too different, where it is achieved 57 % of phenolics removal.

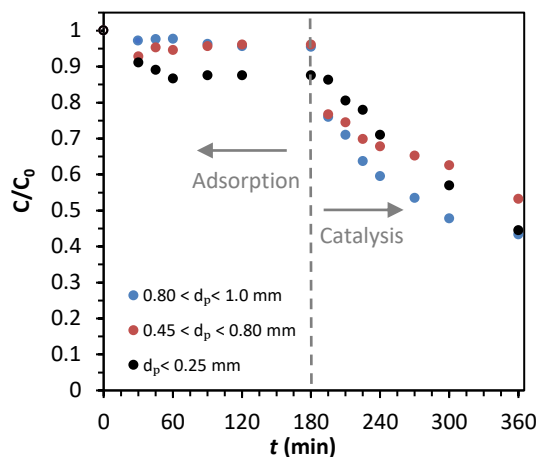


Figure 4.2 Dimensionless concentration of all phenolic compounds (C/C_0) during the adsorption and catalytic processes using catalysts with different particle sizes (d_p). Experimental conditions: SYNTHETIC-1 solution, $[CAT] = 0.5 \text{ g L}^{-1}$, $[H_2O_2] = 0.5 \text{ g L}^{-1}$, $T = 25 \text{ }^\circ\text{C}$, and $pH = 3.6$.

Besides the evaluation of the phenolic compounds, it was also studied the H_2O_2 consumption and TOC removal during the catalytic reaction, see figure 4.4. It should be noted that figures beginning at $t = 180 \text{ min}$ only depict the oxidation process (for brevity, the adsorptive process alone was omitted).

Looking into figure 4.3 (a), the H_2O_2 consumption values are relatively low, ranging 23 to 31 % at the end of the process. The result is explained by the nature of the solution which leads to a competition for the available active sites, i.e., the presence of phenolic compounds creates competition to H_2O_2 molecules resulting in a decrease of oxidant consumption (Pinho et al., 2020).

In figure 4.3 (b) it is observed a low TOC removal for all different catalyst sizes, which might be a result of intermediate products formation and their nature, but also their accumulation in the solution, hindering the further oxidation (Duarte, 2013). The intermediates, usually carboxylic acids and other derivatives, interact with the catalyst causing iron - complexes, diminishing the oxidative potential and phenolics degradation (Esteves et al., 2020; Najjar et al., 2009).

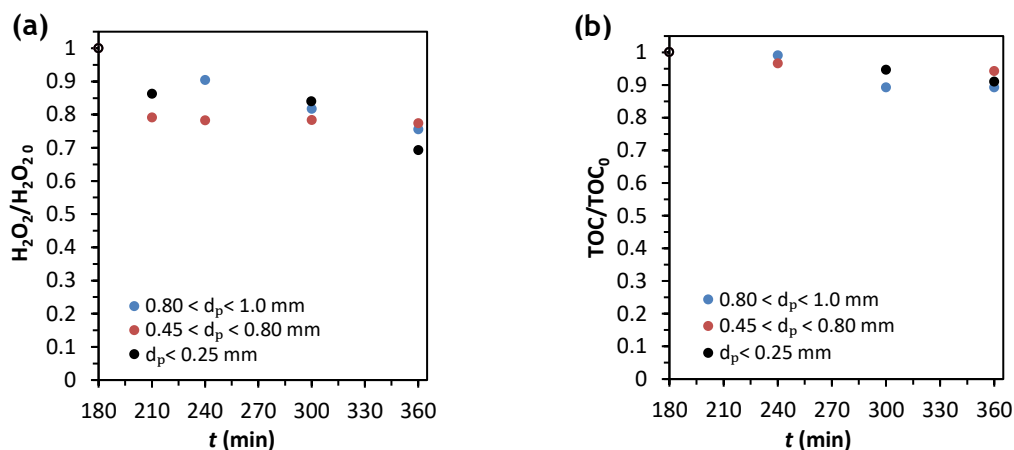


Figure 4.3 (a) Consumption of oxidant and (b) TOC removal during catalysis using catalysts with different particle sizes (d_p). Experimental conditions: SYNTHETIC-1 solution, $[CAT] = 0.5 \text{ g L}^{-1}$, $[H_2O_2] = 0.5 \text{ g L}^{-1}$, $T = 25 \text{ }^\circ\text{C}$, and $pH = 3.6$.

In figure 4.4 it is presented a summary of the final results of the whole process for the range of particle sizes evaluated. It is evident the similarity of TPh and TOC removals regardless of the different particle sizes (the difference between the results is about 8-10 %). This result indicates that, for the range studied, the catalytic reaction is not greatly influenced by the internal mass transfer phenomena (absence of internal resistances to mass transfer - i.e., species diffusion within the catalyst particles is not rate-controlling).

Another important parameter studied, and presented in figure 4.4, was the iron concentration in solution after each experiment. The evaluation of this parameter gives an indication of the iron leaching from the catalysts, and therefore its stability and potential reusability in Fenton-like reactions. As shown in figure 4.4, after 360 min, the obtained leaching values are under 2.5 wt.% (corresponding to 0.679 mg L^{-1} of Fe in solution), thus suggesting a good stability of the catalysts used, also indicating that the contribution of the homogenous catalytic reaction (i.e., promoted by dissolved iron ions in solution) is not predominant in the results.

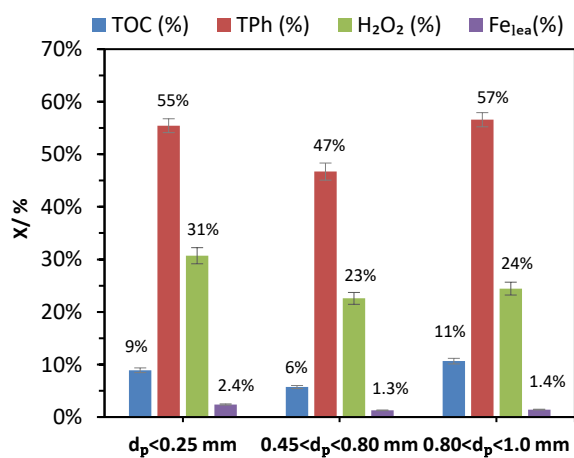


Figure 4.4 Removal of TOC and phenolic compounds (TPh) (%), H_2O_2 consumption (%), and Fe leaching (wt.%) after 180 min of adsorption and 180 min of catalysis. Experimental conditions: SYNTHETIC-1 solution, $[CAT] = 0.5 \text{ g L}^{-1}$, $[H_2O_2] = 0.5 \text{ g L}^{-1}$, $T = 25 \text{ }^\circ\text{C}$, and $pH = 3.6$. Error bars were obtained from the standard errors for a confidence level of 95 %.

4.1.2 Influence of the solution's composition

From the previous results, it is possible to conclude that the particle size influence was negligible. In that sense, the catalyst with the higher particle size was selected for further studies due to the easiness of catalyst recovery, thus minimizing the associated load losses after each run. Moreover, for a possible implementation in a continuous packed-bed reactor, such larger particle size provides smaller pressure drops. Further experiments were performed to study the impact of the solution's composition, using three distinct synthetic solutions comprising five different phenolic compounds (cf. table 3.1) and initial concentration of 350 mg L^{-1} (70 mg L^{-1} each), corresponding to TOC values in the range of $203.3 - 212.8 \text{ mg L}^{-1}$. The idea behind was to check the performance of the catalytic process when dealing with different solutions, having more or less refractory compounds on its composition.

As seen in table 3.1, SYNTHETIC-1 and SYNTHETIC-2 solutions both contain 3 phenolic compounds in common (vanillic, caffeic, and gallic acids), which explains the similarity in the phenolic removal, 57 % and 54 %, respectively (figure 4.5). Rossi et al.(2014) concluded that solutions comprising more phenolic acids present higher COD and TPh removals due to a co-oxidation phenomenon which enhances the process efficiency.

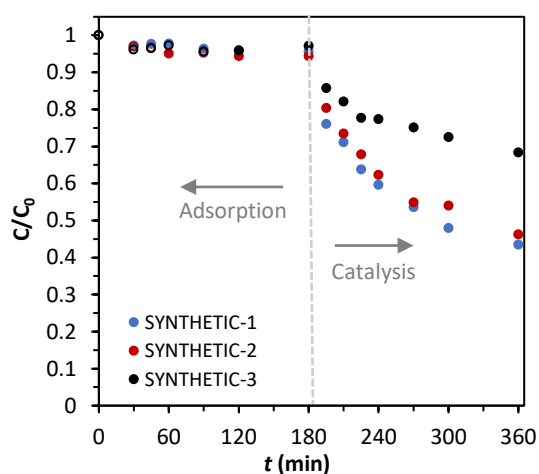
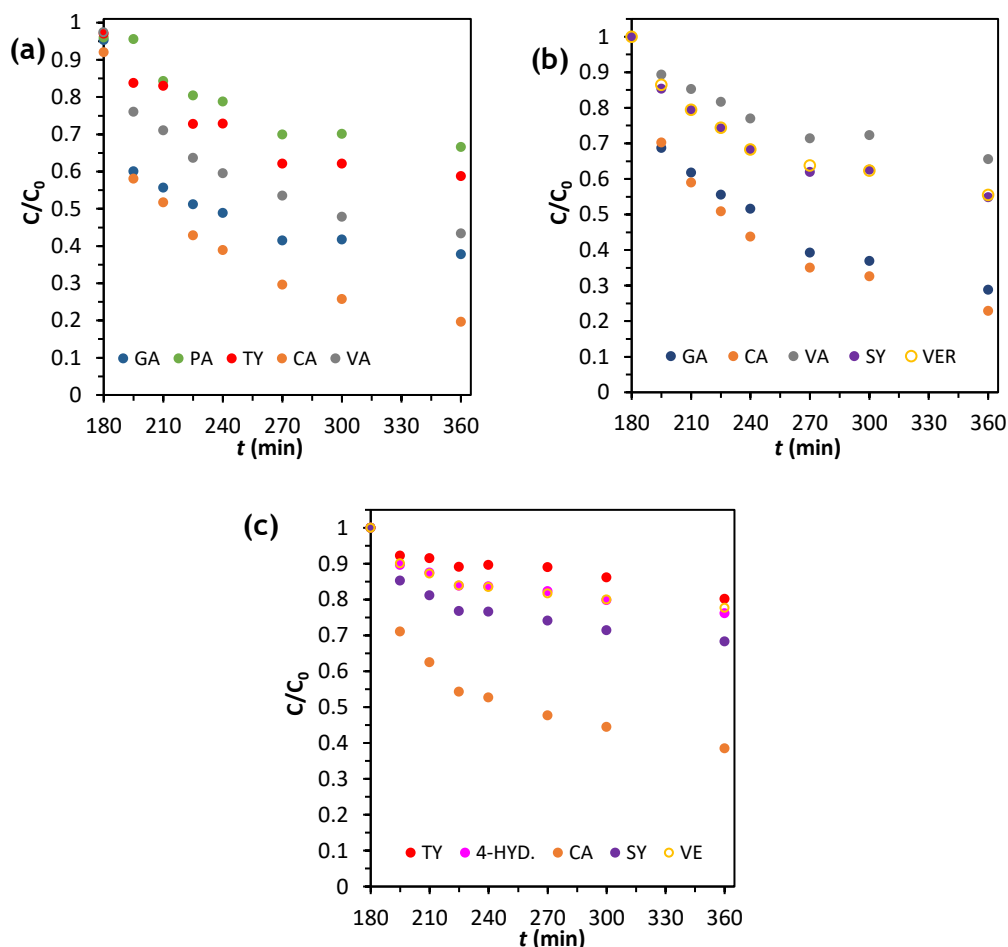


Figure 4.5 Dimensionless concentration of all phenolic compounds (C/C_0) during the adsorption and catalytic processes using different solution's compositions. Experimental conditions: $0.80 < d_p < 1.0 \text{ mm}$, $[CAT] = 0.5 \text{ g L}^{-1}$, $[H_2O_2] = 0.5 \text{ g L}^{-1}$, $T = 25 \text{ }^\circ\text{C}$, and $\text{pH} = 3.6 - 3.8$.

Looking into figure 4.6, the removal of phenolic compounds is clearly favored in SYNTHETIC-1 and 2, as previous stated, while for SYNTHETIC-3 smaller removals were observed (with removals ranging from 20 to 32 % for all compounds, except caffeic acid). The low removals of the phenolic compounds might be a result of a refractory species production. Mantzavinos (2003) work on the removal of benzoic acid derivatives using synthetic effluent and Fenton's process with $[C_0] = 300 \text{ mg L}^{-1}$, $[H_2O_2] = 1500 \text{ mg L}^{-1}$ and $[Fe^{2+}] = 60 \text{ mg L}^{-1}$ concluded that compounds containing -OH groups are more susceptible to oxidation and the increase of these groups increases this effect, while benzoic acid derivatives (protocatechuic, p-hydroxybenzoic

acids) and methoxylated groups (veriatric and syringic acids) present a higher resistance to oxidation. A similar conclusion was drawn by Amor et al. (2015) when treated OMW using Fenton's reagent and anaerobic process using $[\text{COD}_0] = 92.5 \text{ g L}^{-1}$, $[\text{H}_2\text{O}_2] = 0.55 \text{ mol L}^{-1}$ and $[\text{Fe}^{2+}] = 0.0367 \text{ mol L}^{-1}$ at $T = 30 \text{ }^\circ\text{C}$ in the end the authors obtained a low COD conversion (17.6 %) which was explained by the formation of smaller molecules (intermediates) as a result of partial oxidation. The influence of composition in H_2O_2 consumption and TOC removal are shown in appendix B.2.



CA - Caffeic acid; VA - Vanillic acid; GA - Gallic acid; TY - Tyrosol; PA - Protocatechuic acid;
SY - Syringic acid; VER - Veratric acid; 4-HYD - 4-Hydroxybenzoic acid

Figure 4.6 Removal of the individual phenolic compounds (C/C_0) over time using different solution's compositions (a) SYNTHETIC-1, (b) SYNTHETIC-2, (c) SYNTHETIC-3. Experimental conditions: $0.80 < d_p < 1.0 \text{ mm}$, $[\text{CAT}] = 0.5 \text{ g L}^{-1}$, $[\text{H}_2\text{O}_2] = 0.5 \text{ g L}^{-1}$, $T = 25 \text{ }^\circ\text{C}$, and $\text{pH} = 3.6 - 3.8$.

Considering the results presented in figure 4.7, it can be concluded that solutions SYNTHETIC-1 and SYNTHETIC-2 present the best phenolic (57 % and 54 %, respectively) and TOC removals (11 % and 9 %, respectively), while the SYNTHETIC-3 solution presents the lowest values (32 % and 3 %). As stated before, one possible reason for the overall low performances is the production of low molecular weight organic acids such as oxalic, maleic, and acetic acids that

form organic complexes with Fe^{3+} interfering with the regeneration of $\text{Fe}^{2+}/\text{Fe}^{3+}$ (equations 2.3.3 and 2.3.4) and subsequently decrease H_2O_2 consumption, HO^\bullet radical production and mineralization (Ma et al., 2006). The lower performances with SYNTHETIC-3 solution are ascribed to its composition, with more refractory compounds, as stated above.

Regarding the iron leaching values, they remained low in all cases, being 2.4 wt.% the maximum, which means that the catalyst remains stable during the process and guarantees an efficient reusability.

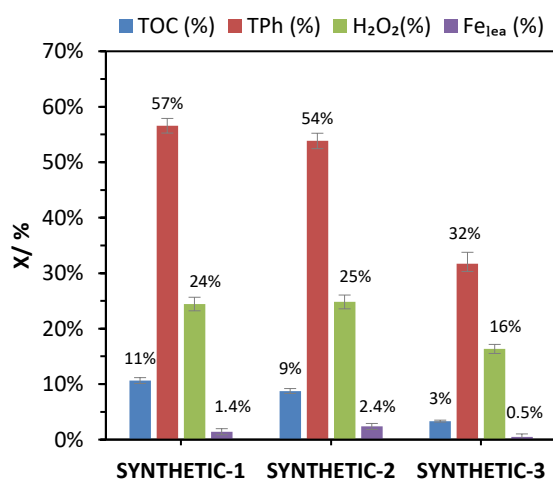


Figure 4.7 Removal of TOC and phenolic compounds (TPh) (%), H_2O_2 consumption (%), and Fe leaching (wt.%) after 180 min of adsorption and 180 min of catalysis. Experimental conditions: $0.80 < d_p < 1.0$ mm, $[\text{CAT}] = 0.5 \text{ g L}^{-1}$, $[\text{H}_2\text{O}_2] = 0.5 \text{ g L}^{-1}$, $T = 25$ °C, and $\text{pH} = 3.6 - 3.8$. Errors bars were obtained from the standard errors for a confidence level of 95 %.

4.1.3 Influence of the catalyst concentration

With the previous experiments it was concluded that SYNTHETIC-1 solution presents better mineralization values, high phenolic removals, and a low level of Fe leaching, which translates into a higher stability and catalytic performance; and thus this solution was preferential to be used in the last set of tests. The influence of the catalyst's concentration was the last parameter studied, using catalyst's concentrations of 0.5 g L^{-1} , 1.5 g L^{-1} and 2.5 g L^{-1} - figure 4.8.

In figure 4.8, the increase in the catalyst concentration led to a clear improvement of the adsorption results. The increase of catalyst load leads to a high number of active sites increasing the phenolic adsorption; however, during the catalytic experiments, the performances reached are nearly the same, particularly after 240 min, whatever the catalyst load, in the range tested.

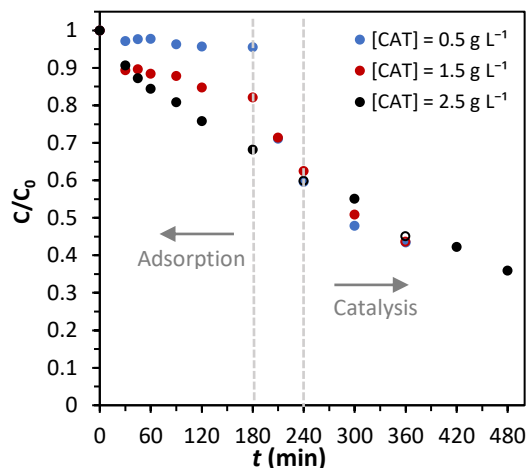


Figure 4.8 Dimensionless concentration of all phenolic compounds (C/C_0) during the adsorption and catalytic processes using different catalyst concentrations. Experimental conditions: SYNTHETIC-1 solution, $0.80 < d_p < 1.0$ mm, $[H_2O_2] = 0.5$ g L⁻¹, $T = 25$ °C, and $pH = 3.6$. For $[CAT] = 2.5$ g L⁻¹, catalysis starts at $t = 240$ min.

In figures 4.9 (a) and (b) are showed the effect of the catalyst load in the H_2O_2 consumption and TOC removal, respectively. The increase of catalyst load shows a positive effect in TOC removals and H_2O_2 consumption. According to Zhang et al. (2019), increasing the amount of Fe^{2+} , increases the consumption of H_2O_2 and subsequently the HO^\bullet radical production, improving the degradation efficiency. Nevertheless, it is necessary to optimize the catalyst concentration since the excessive amount can lead to an increase of operational costs, but more importantly to the enhancement of the scavenging effect (cf. 2.3.5).

Domingues et al. (2019) tested the increase of catalyst load as a parameter to improve the efficiency of the heterogeneous Fenton process; for that the authors used catalyst loads from 0.5 g L⁻¹ to 1.0 g L⁻¹ being verified an increase in the reaction efficiency; however, when the catalyst load was increased above 1.0 g L⁻¹, it was verified a scavenger effect. Another study made by the same authors using the Fenton's process with iron concentrations between 0.1-3.0 g L⁻¹, $[H_2O_2] = 4$ g L⁻¹ at $pH = 3$ for 60 min, showed similar conclusions, i.e. higher COD removals (40 %) using catalyst loads up to 2.5 g L⁻¹, while higher concentrations demonstrated a detrimental effect on the catalytic efficiency, again confirming the scavenging effect as a consequence of the excessive iron load (Domingues et al., 2021).

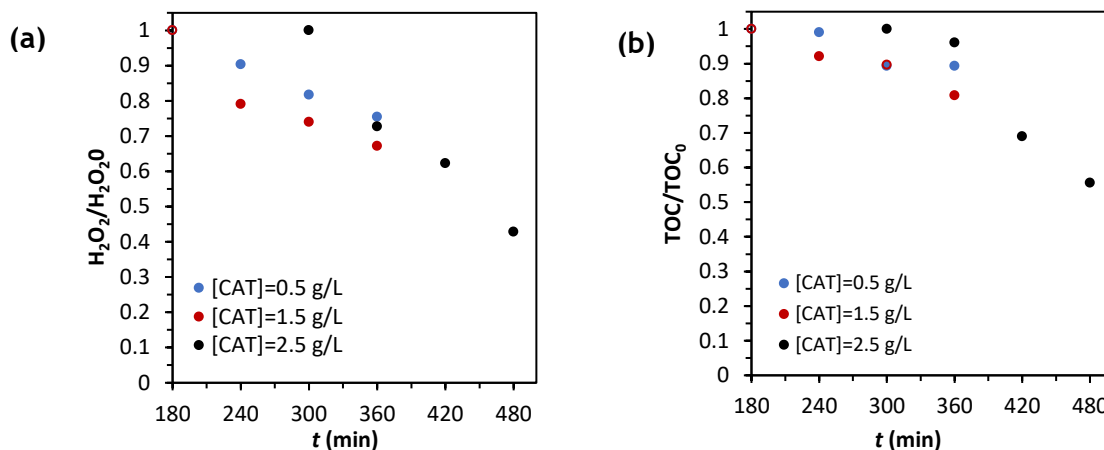


Figure 4.9 (a) Consumption of oxidant and (b) TOC removal during the catalytic process using different catalyst concentrations. Experimental conditions: SYNTHETIC-1 solution, $0.80 < d_p < 1.0$ mm, $[H_2O_2] = 0.5$ g L⁻¹, $T = 25$ °C, and $pH = 3.6$. For $[CAT] = 2.5$ g L⁻¹, catalysis starts at $t = 240$ min.

In appendix B.3 are presented the phenolic removal over time for the different catalyst concentrations and it can be noticed that increasing catalyst load led the full degradation of caffeic (CA) and gallic (GA) acids. Another positive result was the increase of the protocatechuic acid (PA) degradation, reaching 52 % of removal, however, it is observed a smaller degradation of vanillic acid (37 %), one possible reason for this outcome might be connected to the absence of an electrophilic attack caused by a low number of EDG groups, and the presence of methoxy (O - CH₃) group which gives a higher resistance to degradation, as seen earlier (Esteves et al., 2020; Mantzavinos, 2003).

Overall, the final results showed a positive effect with the catalyst load increase attaining 31 % of mineralization, 58 % of phenolics removal and 38 % of H₂O₂ consumption using a catalyst concentration of 2.5 g L⁻¹ (figure 4.10). However, the increase of catalyst load (5 X) does not show significant improvements in the catalytic performance; one possible explanation is the Fe leached during the reaction that increase from 2.4 % to 8 %. Usually, the increase of this parameter leads to catalyst deactivation, and an increase of instability during the reaction (Zazo et al., 2006). All together these results lead to the conclusion that 2.5 g L⁻¹ is an excessive catalyst concentration.

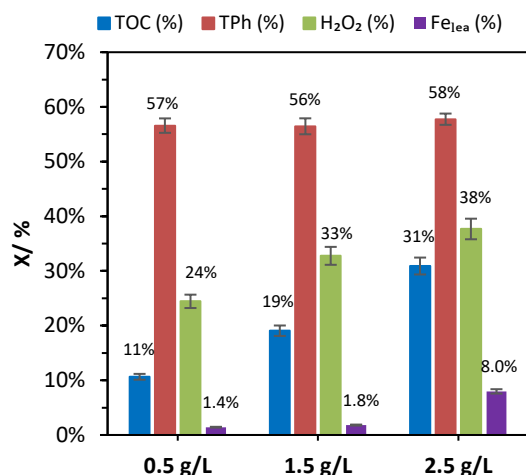


Figure 4.10 Removal of TOC and phenolic compounds (TPh) (%), H₂O₂ consumption (%), and Fe leaching (wt.%) after 180/240 min of adsorption + 180/120 min of catalysis. Experimental conditions: SYNTHETIC-1 solution, $0.80 < d_p < 1.0$ mm, $[H_2O_2] = 0.5$ g L⁻¹, $T = 25$ °C, and $pH = 3.6$. Errors bars were obtained from the standard errors for a confidence level of 95 %. For $[CAT] = 2.5$ g L⁻¹, the catalytic process starts at $t = 240$ min.

4.2 Real Olive Mill Wastewater Treatment

In this section, real effluents were used, provided by a local facility, operating a 3-phase mill, with COD = 1094.4 mg L⁻¹, TOC = 527.4 mg L⁻¹, and TPh = 47.7 mg L⁻¹ (cf. table 3.3). During these experiments, it was studied the effect of catalyst load and temperature using previously saturated catalysts.

4.2.1 Effect of catalyst load

As seen before, one way of optimizing the heterogeneous Fenton process is to determine the right amount of catalyst load to increase the HO[•] radical production and avoid the scavenger effect. In figure 4.11 (a) are presented the TPh removal values using three different catalyst loads; for that, it was used the Folin-Ciocalteu method, where gallic acid was used as the standard component and results are reported as mg GA_{eq} L⁻¹.

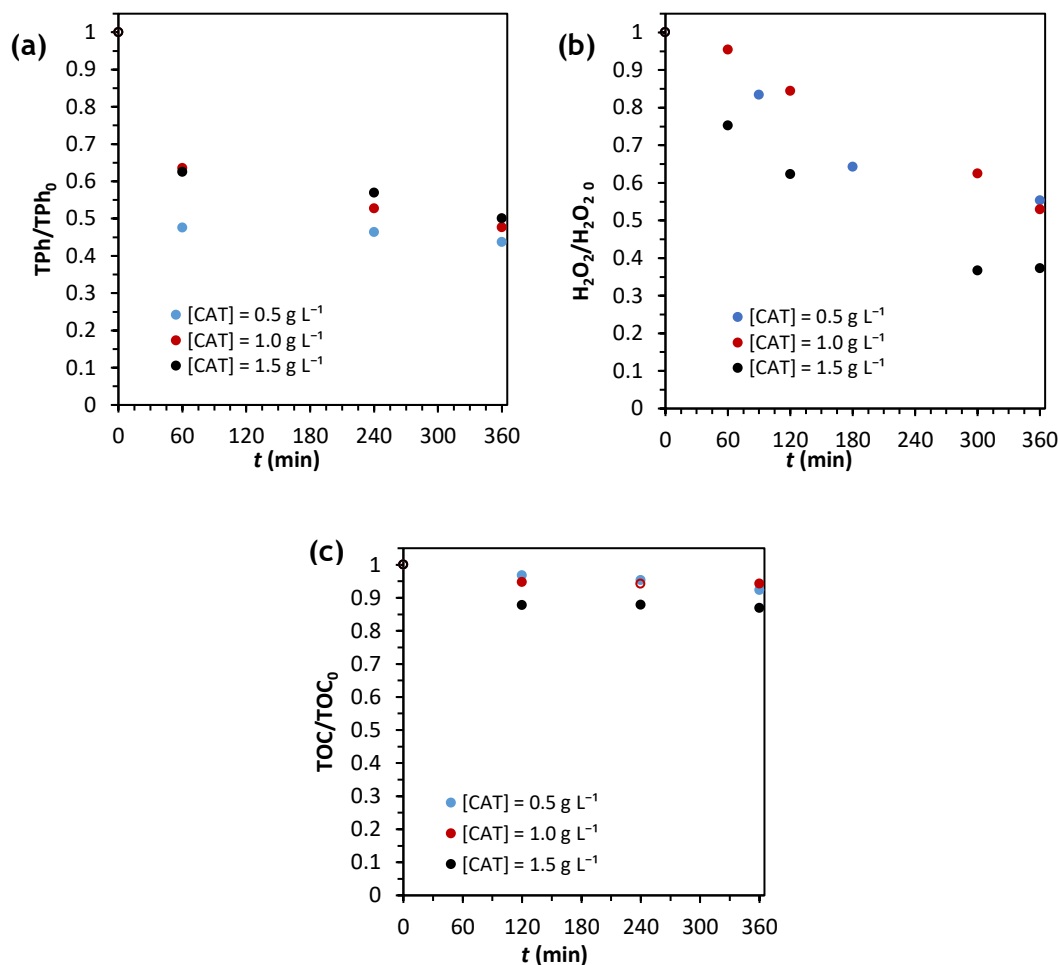


Figure 4.11 (a) TPh removal (b) Consumption of oxidant and (c) TOC removal in real effluents using different concentrations of catalyst. Experimental conditions: $0.80 < d_p < 1.0$ mm, $[H_2O_2] = 0.5$ g L⁻¹, $T = 24$ °C, $pH = 3.4$.

Overall, the TPh removals were satisfactory, reaching values close to 60 % after 360 min; it is also noticeable an identical performance of the different catalyst concentrations (figure 4.11 a), which was not expected since the increase of catalytic load also increases the amount of Fe²⁺ leading to a raise in phenolic degradation (Maduna et al., 2018). This outcome might be explained due to the complex composition of the OMW which causes the production of intermediates showing a negative impact on the efficiency, as stated before. Still, the scavenging effect of excessive catalyst concentrations has to be taken into account.

Despite the unexpected results for the TPh removals, H₂O₂ consumption showed 63 % of oxidant consumption for the concentration of 1.5 g L⁻¹ (figure 4.11 b) while 0.5 g L⁻¹ results in 45 % of consumption reinforcing the effect of the iron load. During these experiments, the obtained TOC removals were low, figure 4.11 c, which might be a result of the initial composition of the complex effluent and the decrease of oxidant levels, which reveals to be insufficient to degrade high concentration loads (M. hui Zhang et al., 2019). A general point of view of the overall performances reached is presented in figure 4.12 where it is also displayed the results of COD measurements.

Figure 4.12 shows the increase of H_2O_2 consumption due to increase of catalyst load, which almost did not affect TOC, COD and TPh removals, since the use of 3 times more catalyst only led to an increase of 5 % of TOC and 4% of COD removals. According to Zazo et al. (2006) one possible explanation may be a surface blockage caused by the formation of polymeric layer as a result of intermediates production which causes a diminished porosity and superficial area. Another possibility is the development of parallel reactions between the Fe^{3+} species (in excess) and HO^\bullet radicals (cf. equation 2.3.5) also known as scavenging effect (Ramirez et al., 2007). According to the obtained results it is possible to conclude that the efficient catalyst load for the treatment of real OMW is 0.5 g L^{-1} since the increase of catalyst load did not show bigger improvements.

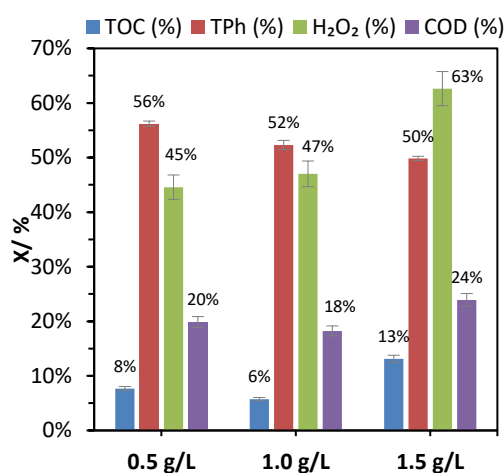


Figure 4.12 Removal of TOC, phenolic compounds (TPh), COD (%) and H_2O_2 consumption (%) in real effluents using different catalyst concentrations. Experimental conditions: $0.80 < d_p < 1.0 \text{ mm}$, $[\text{H}_2\text{O}_2] = 0.5 \text{ g L}^{-1}$, $T = 24 \text{ }^\circ\text{C}$, $\text{pH} = 3.4$. Errors bars were obtained from the standard errors for a confidence level of 95 %.

4.2.2 Effect of temperature

Temperature is another important factor to optimize when using the CWPO process. Usually, near room temperatures ($25 \text{ }^\circ\text{C}$) or temperatures until $50 \text{ }^\circ\text{C}$ are selected, due to energy costs and good performances, however, in some cases, CWPO processes can be used until $160 \text{ }^\circ\text{C}$ (Márquez et al., 2018). In this work, the effect of the temperature was tested using near room ($25 \text{ }^\circ\text{C}$) and higher temperatures ($50 \text{ }^\circ\text{C}$ and $75 \text{ }^\circ\text{C}$) with a real effluent.

The final values of the oxidation process are presented in figure 4.13 being clearly evident that the temperature increase had a positive impact in all the measured values, being obtained 56 %, 63 % and 93 % of phenolic compound removals, at 25, 50 and $75 \text{ }^\circ\text{C}$, respectively - figure 4.13 (a). The increase of temperature influences the kinetics of all reactions according to Arrhenius law, cf. equation 2.4.1, which means that an increase of temperature enhances the H_2O_2 decomposition, the formation of hydroxyl radicals and enhances the degradability of the organic compounds (Márquez et al., 2018).

According to Azabou et al. (2010) study, using 0.5 g L^{-1} of catalyst, 0.02 M of H_2O_2 and 1.25 g L^{-1} of phenol concentration under 8 hours, wherein it was tested the effect of temperature in the CWPO process at three different temperatures ($25 \text{ }^\circ\text{C}$, $50 \text{ }^\circ\text{C}$ and $70 \text{ }^\circ\text{C}$), in the end it was obtained COD reductions of 37 %, 50 % and 69 % and phenol reductions of 54 %, 83 % and 100 % were obtained, respectively. Zazo et al. (2011) also studied the effect of temperature on Fenton's reaction, using temperatures between $25\text{-}130^\circ \text{C}$, $[\text{Phenol}] = 100 \text{ mg L}^{-1}$, $[\text{Fe}^{2+}] = 10 \text{ mg L}^{-1}$ and $[\text{H}_2\text{O}_2] = 500 \text{ mg L}^{-1}$. The TOC removals obtained were 28 %, 54 %, 58 % and 77 % using $25 \text{ }^\circ\text{C}$, $50 \text{ }^\circ\text{C}$, $70 \text{ }^\circ\text{C}$ and $90 \text{ }^\circ\text{C}$, respectively. The authors concluded that the increase of temperature enhanced the H_2O_2 decomposition, HO^\bullet radical production and phenol mineralization.

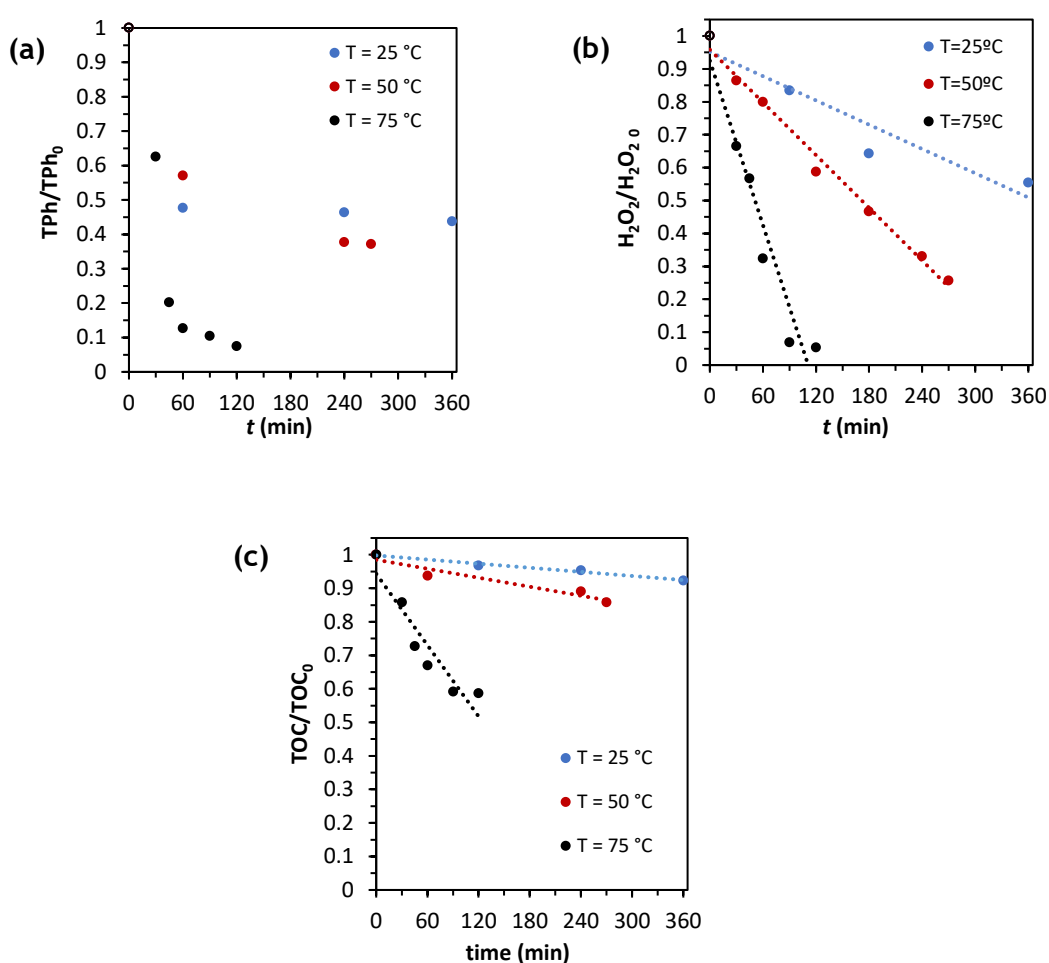


Figure 4.13 (a) TPh removal (b) consumption of oxidant and (c) TOC removal in real effluents at different temperatures. Experimental conditions: $0.80 < d_p < 1.0 \text{ mm}$, $[\text{CAT}] = 0.5 \text{ g L}^{-1}$, $[\text{H}_2\text{O}_2] = 0.5 \text{ g L}^{-1}$, $\text{pH} = 3.4$. Catalytic results ended at $t = 270 \text{ min}$ using $T = 50 \text{ }^\circ\text{C}$ and ended at 120 min for $T = 75 \text{ }^\circ\text{C}$.

Figure 4.14 shows the impact of the increase in the reaction temperature in all parameters assessed; an overall positive impact with the increase of temperature is noticed, reaching 74 % and 95 % of H_2O_2 consumption, and 63 % and 93 % of TPh removals when operating at higher temperatures (50 °C and 75 °C, respectively). The small increase of TOC values, from 25 °C to 50 °C, might be a result of the complex composition of OMW and the production of intermediates, as already stated. However, when the temperature increases to 75 °C, these intermediates start to be oxidized and mineralized, being reached a value of 41% in TOC removal. Still, COD reduction as high as 58% was reached at the highest temperature tested. It is finally worth mentioning that the positive effect of the reaction temperature in all parameters assessed is not the only positive outcome; one should also remark that this was reached at significantly smaller reaction times, which was reduced from 360 min to 270 min and down to 120 min when temperature was respectively increased from 25 to 50 and to 75 °C; so, much higher performances are reached at 75 °C vs. 25 °C requiring only 1/3 of the process time. Of course, this positive impact on reaction kinetics is at cost of higher energy requirements, which in some olive oil industries might be free since olive paste needs to be washed at high temperatures prior to oil separation (Amor et al., 2019).

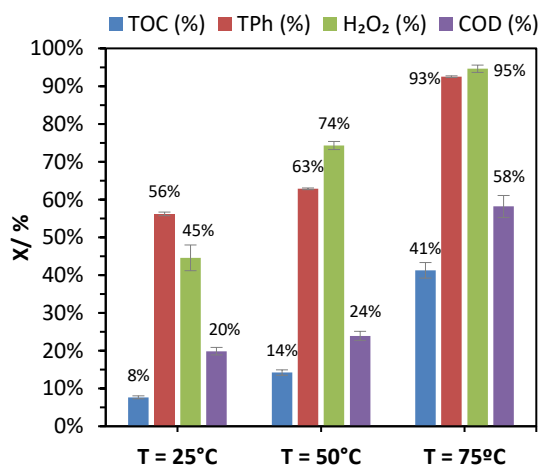


Figure 4.14 Removal of TOC, phenolic compounds (TPh) and COD (%), H_2O_2 consumption (%) in real effluents at different temperatures. Experimental conditions: $0.80 < d_p < 1.0$ mm, $[CAT] = 0.5$ g L^{-1} , $[H_2O_2] = 0.5$ g L^{-1} , pH = 3.4. Errors bars were obtained from the standard errors for a confidence level of 95 %.

4.2.3 Catalyst reutilization

Reutilization of the catalyst is another important operational parameter in order to guarantee industrial applications (Cruz Gonzalo, 2017; X. Zhang et al., 2020). To evaluate this parameter, four consecutive experiments lasting 360 min each were performed ($[CAT] = 0.5 \text{ g L}^{-1}$, $[H_2O_2] = 0.5 \text{ g L}^{-1}$, $pH = 3.4$ at $T = 75 \text{ }^\circ\text{C}$). After each cycle the catalyst was recovered by filtration, rinsed with distilled water, dried and reused in a subsequent run.

Figure 4.15 shows the material's catalytic performance after each cycle. Overall, the TPh removal and H_2O_2 consumption values were maintained above 90 % and 95 %, respectively. Considering the catalytic results obtained under these experimental conditions, it can be said that the selected catalyst has shown promising reusability features for the treatment of olive mill wastewater.

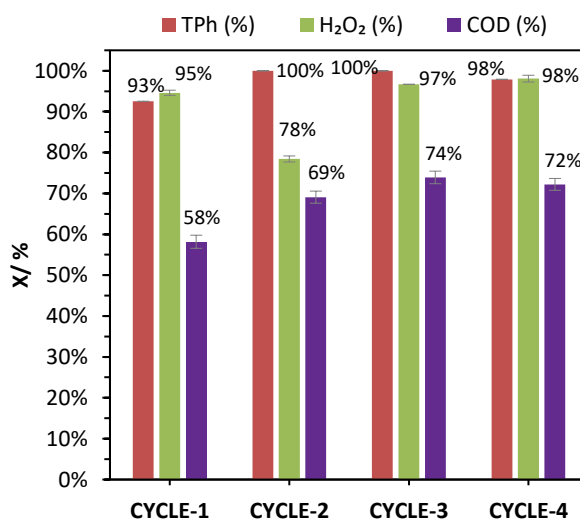


Figure 4.15 Removal of phenolic compounds (TPh), COD (%) and H_2O_2 consumption (%) in 4 consecutive cycles using a real effluent. Experimental conditions: $0.80 < d_p < 1.0 \text{ mm}$, $[CAT] = 0.5 \text{ g L}^{-1}$, $[H_2O_2] = 0.5 \text{ g L}^{-1}$, $pH = 3.4$. CYCLE-1 ends at 120 min, the remained cycles ended at 180 min. Errors bars were obtained from the standard errors for a confidence level of 95 %.

5 Conclusions

The developed work presented in this dissertation focused on the treatment of OMW effluents, identified as being toxic and hazardous and usually difficult to handle. In order to treat these effluents, the heterogeneous Fenton process with carbon-based catalysts (OSAC-Fe) is used as an effective and low-cost treatment alternative. First, synthetic solutions were employed to study the influence of some operational parameters in the heterogeneous Fenton process, such as, the catalyst particle size, synthetic solution initial composition, and catalyst concentration. Afterwards, the impact of the temperature and catalyst load in real OMW treatment was studied.

In the first set of experiments, it was concluded that the particle size does not influence the catalytic process due to the similar results obtained for the different particle size ranges, with overall TOC removals of 9 %, 6 % and 11 % for the smaller, intermediate and larger catalyst particle ranges, respectively, after 360 min (180 min of adsorption and 180 min of catalysis). Therefore, the biggest particle size range ($0.80 < d_p < 1.0$ mm) was selected for the other experiments due to the easiness of recovery. Afterwards, the influence of the initial composition of the synthetic OMW was studied, where 3 different compositions with an initial concentration of 350 mg/L were used. It was observed an influence of the composition in the catalytic oxidation since some phenolic compounds are easier to degrade (80 % for caffeic and 62 % for gallic acids) and others present a resistance to degradation or formation of refractory intermediates. The catalyst concentration was also studied and showed a positive influence in the catalytic process when it was increased from 0.5 g L^{-1} to 2.5 g L^{-1} since mineralization degree increased from 11 % to 31 %; however, an increase of iron leaching (8 %) with the increase of catalyst load was also detected.

In the last set of experiments, it was studied the effect of the catalyst load and temperature using a real OMW provided by a local industry. First, it was concluded that the catalyst concentration of 0.5 g L^{-1} was enough to obtain 8 % of TOC, 56 % of TPh and 20 % of COD removals, and 45 % of H_2O_2 consumption at the end of the process. Higher catalyst doses did not improve noticeably the process performance, possibly due to scavenging effects (i.e., parallel undesired reactions). Lastly, a significant positive impact was observed when the temperature was increased, since degradability of the organic compounds were enhanced, resulting in 95% depletion of phenolic compounds, 41 % of TOC removal and reduction of COD by 58 % in only 120 min at $T = 75 \text{ }^\circ\text{C}$. Still, it was also detected a decrease in reaction time. Finally, it was found that the catalyst remains stable and can be reused in, at least, 4 consecutive reaction cycles.

6 Assessment of the work done

6.1 Objectives Achieved

The developed work was focused on 3 main goals: i) the use of organic residues from the olive oil industry as potential catalysts in the heterogonous Fenton reaction as an adequate process to handle the OMW discharges, ii) guarantee the maximum performance and stability of the OS-AC-Fe catalysts, and iii) improve the Fenton's reaction by optimizing the main operational parameters. Overall, it was demonstrated the efficiency of the OS-AC-Fe catalysts since acceptable values of phenolic removal, oxidant consumption and mineralization were observed. It was also guaranteed the maximum performance, reasonable stability of the selected catalyst and the optimization of Fenton's reaction due to the improvement of performance by changing the operational parameters, which resulted in an increase of mineralization, and a minimum amount of Fe leached. Despite of the increase in iron leaching using a catalyst concentration of 2.5 g L^{-1} , overall, it was visible an increase in the performance of the heterogeneous Fenton reaction.

6.2 Final Assessment

The main goal of providing an efficient OMW treatment using the heterogeneous Fenton process was achieved. Despite the overall satisfactory results obtained, it should have been better clarified the effect of the catalyst load by testing other concentrations. Still, it should also be identified the main intermediates formed, and their impact on the overall heterogeneous Fenton reaction. Stability tests are also recommended as a key issue for future work.

7 References

- Alver, A., Baştürk, E., Kiliç, A., & Karataş, M. (2015). Use of advance oxidation process to improve the biodegradability of olive oil mill effluents. *Process Safety and Environmental Protection*, 98, 319-324. <https://doi.org/10.1016/j.psep.2015.09.002>
- American Public Health Association (APHA). (1999). Section 5310: Total organic carbon (TOC). *Standard Methods for the Examination of Water and Wastewater*, 1.
- American Public Health Association (APHA), American Water Works Association, (AWWA), & World Economic Forum, (WEF). (1998). Standard Methods for the Examination of Water and Wastewater. In *Water Research*. [https://doi.org/10.1016/0043-1354\(82\)90249-4](https://doi.org/10.1016/0043-1354(82)90249-4)
- Amor, C., Lucas, M. S., García, J., Dominguez, J. R., De Heredia, J. B., & Peres, J. A. (2015). Combined treatment of olive mill wastewater by Fenton's reagent and anaerobic biological process. *Journal of Environmental Science and Health - Part A Toxic/Hazardous Substances and Environmental Engineering*, 50(2), 161-168. <https://doi.org/10.1080/10934529.2015.975065>
- Amor, C., Marchão, L., Lucas, M. S., & Peres, J. A. (2019). Application of advanced oxidation processes for the treatment of recalcitrant agro-industrial wastewater: A review. *Water (Switzerland)*, 11(2). <https://doi.org/10.3390/w11020205>
- Azabou, S., Najjar, W., Bouaziz, M., Ghorbel, A., & Sayadi, S. (2010). A compact process for the treatment of olive mill wastewater by combining wet hydrogen peroxide catalytic oxidation and biological techniques. *Journal of Hazardous Materials*, 183(1-3), 62-69. <https://doi.org/10.1016/j.jhazmat.2010.06.104>
- Babić, S., Malev, O., Pflieger, M., Lebedev, A. T., Mazur, D. M., Kužić, A., Čož-Rakovac, R., & Trebše, P. (2019). Toxicity evaluation of olive oil mill wastewater and its polar fraction using multiple whole-organism bioassays. *Science of the Total Environment*, 686, 903-914. <https://doi.org/10.1016/j.scitotenv.2019.06.046>
- Barroso-Bogeat, A., Alexandre-Franco, M., Fernández-González, C., & Gómez-Serrano, V. (2020). Surface morphological characterization of activated carbon-metal (hydr)oxide composites: some insights into the role of the precursor chemistry in aqueous solution. *Journal of Dispersion Science and Technology*, 41(12), 1743-1753. <https://doi.org/10.1080/01932691.2019.1635889>
- Commission, E. (2006). Directive 2006/11/EC, (old) Pollution by certain dangerous substances. *Official Journal of the European Union*, 2455, L 64/52-L 64/59.
- Cruz Gonzalo, A. (2017). *Synthesis and performance of heterogeneous catalysts for Fenton-like and photo-Fenton-like reactions at circumneutral pH*. Universitat de Barcelona.
- Demiray, S., Piccirillo, C., Rodrigues, C. L., Pintado, M. E., & Castro, P. M. L. (2011). Extraction of valuable compounds from Ginja cherry by-products: Effect of the solvent and antioxidant properties. *Waste and Biomass Valorization*, 2(4), 365-371. <https://doi.org/10.1007/s12649-011-9088-0>
- Diário da República. (1998). Decrete-Law no. 236/98. SÉRIE-A, DIÁRIO DA REPÚBLICA – I, N.o 176, 3676-3722.

- Domingues, E., Assunção, N., Gomes, J., Lopes, D. V., Frade, J. R., Quina, M. J., Quinta-Ferreira, R. M., & Martins, R. C. (2019). Catalytic efficiency of red mud for the degradation of Olive mill wastewater through heterogeneous Fenton's process. *Water (Switzerland)*, 11(6). <https://doi.org/10.3390/w11061183>
- Domingues, E., Fernandes, E., Gomes, J., Castro-Silva, S., & Martins, R. C. (2021). Olive oil extraction industry wastewater treatment by coagulation and Fenton's process. 39(November 2020). <https://doi.org/10.1016/j.jwpe.2020.101818>
- Domingues, E., Gomes, J., Quina, M. J., Quinta-Ferreira, R. M., & Martins, R. C. (2018). Detoxification of olive mill wastewaters by Fenton's process. *Catalysts*, 8(12). <https://doi.org/10.3390/catal8120662>
- Duarte, F. (2013). *Treatment of textile effluents by Fenton-like oxidation processes with carbon-based catalysts* (Issue May).
- Espadas-Aldana, G., Vialle, C., Belaud, J. P., Vaca-Garcia, C., & Sablayrolles, C. (2019). Analysis and trends for Life Cycle Assessment of olive oil production. *Sustainable Production and Consumption*, 19, 216-230. <https://doi.org/10.1016/j.spc.2019.04.003>
- Esteves, B. M., Morales-Torres, S., Maldonado-Hódar, F. J., & Madeira, L. M. (2020). Fitting biochars and activated carbons from residues of the olive oil industry as supports of Fe-catalysts for the heterogeneous Fenton-like treatment of simulated olive mill wastewater. *Nanomaterials*, 10(5), 1-26. <https://doi.org/10.3390/nano10050876>
- Figueiredo, J. L., & Ramôa Ribeiro, F. (2015). *Catálise Heterogénea* (3ª). Fundação Calouste Gulbenkian.
- Fragoso, R. A., & Duarte, E. A. (2012). Reuse of drinking water treatment sludge for olive oil mill wastewater treatment. *Water Science and Technology*, 66(4), 887-894. <https://doi.org/10.2166/wst.2012.267>
- Freedman, J. C. (2012). Biophysical chemistry of physiological solutions. In N. Sperelakis (Ed.), *Cell Physiology Source Book* (4th ed., pp. 3-17). Elsevier Inc. <https://doi.org/10.1016/B978-0-12-387738-3.00001-9>
- Gil, A., Korili, S. A., Trujillano, R., & Vicente, M. A. (2010). Pillared clays and related catalysts. In *Pillared Clays and Related Catalysts*. <https://doi.org/10.1007/978-1-4419-6670-4>
- Hodaifa, G., Ochando-Pulido, J. M., Rodriguez-Vives, S., & Martinez-Ferez, A. (2013). Optimization of continuous reactor at pilot scale for olive-oil mill wastewater treatment by Fenton-like process. *Chemical Engineering Journal*, 220, 117-124. <https://doi.org/10.1016/j.cej.2013.01.065>
- Hudz, N., Yezerska, O., Shanaida, M., Sedláčková, V. H., & Wieczorek, P. P. (2019). Application of the Folin-Ciocalteu method to the evaluation of Salvia sclarea extracts. *Pharmacia*, 66(4), 209-215. <https://doi.org/10.3897/pharmacia.66.e38976>
- International Olive Oil Council. (2018a). *Huiles D' Olive - Olive Oils*. International Olive Oil Council. <http://www.internationaloliveoil.org>
- International Olive Oil Council. (2018b). *Huiles D' Olive - Olive Oils*. *International Olive Oil Council*, June, 2018. <http://www.internationaloliveoil.org>
- Justino, C. I. L., Pereira, R., Freitas, A. C., Rocha-Santos, T. A. P., Panteleitchouk, T. S. L., & Duarte, A.

- C. (2012). Olive oil mill wastewaters before and after treatment: A critical review from the ecotoxicological point of view. *Ecotoxicology*, 21(2), 615-629. <https://doi.org/10.1007/s10646-011-0806-y>
- Kang, Y. W., Cho, M. J., & Hwang, K. Y. (1999). Correction of hydrogen peroxide interference on standard chemical oxygen demand test. *Water Research*, 33(5), 1247-1251. [https://doi.org/10.1016/S0043-1354\(98\)00315-7](https://doi.org/10.1016/S0043-1354(98)00315-7)
- Lafi, W. K., Shannak, B., Al-Shannag, M., Al-Anber, Z., & Al-Hasan, M. (2009). Treatment of olive mill wastewater by combined advanced oxidation and biodegradation. *Separation and Purification Technology*, 70(2), 141-146. <https://doi.org/10.1016/j.seppur.2009.09.008>
- Lucas, M. S., Béltran-Heredia, J., Sanchez-Martin, J., Garcia, J., & Peres, J. A. (2013). Treatment of high strength olive mill wastewater by Fenton's reagent and aerobic biological process. *Environmental Science and Health*, 48(Toxic/Hazardous Substances and Environmental Engineering), 954-962.
- Lucas, M. S., & Peres, J. A. (2009). Removal of COD from olive mill wastewater by Fenton's reagent: Kinetic study. *Journal of Hazardous Materials*, 168(2-3), 1253-1259. <https://doi.org/10.1016/j.jhazmat.2009.03.002>
- Ma, J., Ma, W., Song, W., Chen, C., Tang, Y., Zhao, J., Huang, Y., Xu, Y., & Zang, L. (2006). Fenton degradation of organic pollutants in the presence of low-molecular-weight organic acids: Cooperative effect of quinone and visible light. *Environmental Science and Technology*, 40(2), 618-624. <https://doi.org/10.1021/es051657t>
- Maduna, K., Kumar, N., Aho, A., Wärnå, J., Zrnčević, S., & Murzin, D. Y. (2018). Kinetics of Catalytic Wet Peroxide Oxidation of Phenolics in Olive Oil Mill Wastewaters over Copper Catalysts. *ACS Omega*, 3(7), 7247-7260. <https://doi.org/10.1021/acsomega.8b00948>
- Mantzavinos, D. (2003). Removal of benzoic acid derivatives from aqueous. *Process Safety and Environmental Protection*, 81(March), 99-106.
- Márquez, J. J. R., Levchuk, I., & Sillanpää, M. (2018). Application of catalytic wet peroxide oxidation for industrial and urban wastewater treatment: A review. *Catalysts*, 8(12). <https://doi.org/10.3390/catal8120673>
- Martins, R. C., Amaral-Silva, N., & Quinta-Ferreira, R. M. (2010). Ceria based solid catalysts for Fenton's depuration of phenolic wastewaters, biodegradability enhancement and toxicity removal. *Applied Catalysis B: Environmental*, 99(1-2), 135-144. <https://doi.org/10.1016/j.apcatb.2010.06.010>
- Najjar, W., Azabou, S., Sayadi, S., & Ghorbel, A. (2009). Screening of Fe-BEA catalysts for wet hydrogen peroxide oxidation of crude olive mill wastewater under mild conditions. *Applied Catalysis B: Environmental*, 88(3-4), 299-304. <https://doi.org/10.1016/j.apcatb.2008.11.023>
- Navalon, S., Dhakshinamoorthy, A., & Alvaro, M. (2011). Heterogeneous Fenton Catalysts Based on Activated Carbon and Related Materials. *ChemSusChem*, 1712-1730. <https://doi.org/10.1002/cssc.201100216>
- Neyens, E., & Baeyens, J. (2003). A review of classic Fenton's peroxidation as an advanced oxidation technique. *Journal of Hazardous Materials*, 98(1-3), 33-50. [https://doi.org/10.1016/S0304-3894\(02\)00282-0](https://doi.org/10.1016/S0304-3894(02)00282-0)

- Nieto, L. M., Hodaifa, G., Rodríguez, S., Giménez, J. A., & Ochando, J. (2011a). Degradation of organic matter in olive-oil mill wastewater through homogeneous Fenton-like reaction. *Chemical Engineering Journal*, 173(2), 503-510. <https://doi.org/10.1016/j.cej.2011.08.022>
- Nieto, L. M., Hodaifa, G., Rodríguez, S., Giménez, J. A., & Ochando, J. (2011b). Flocculation-Sedimentation Combined with Chemical Oxidation Process. *Clean - Soil, Air, Water*, 39(10), 949-955. <https://doi.org/10.1002/clen.201000594>
- Ochando-Pulido, J. M., Pimentel-Moral, S., Verardo, V., & Martínez-Ferez, A. (2017). A focus on advanced physico-chemical processes for olive mill wastewater treatment. *Separation and Purification Technology*, 179, 161-174. <https://doi.org/10.1016/j.seppur.2017.02.004>
- Pinho, M. T., Ribeiro, R. S., Gomes, H. T., Faria, J. L., & Silva, A. M. T. (2020). Screening of activated carbons for the treatment of highly concentrated phenol solutions using catalytic wet peroxide oxidation: The effect of iron impurities on the catalytic activity. *Catalysts*, 10(11), 1-14. <https://doi.org/10.3390/catal10111318>
- Queirós, S. A. dos S. (2014). *Tratamento de um efluente corado por oxidação tipo Fenton*.
- Ramirez, J. H., Maldonado-Hódar, F. J., Pérez-Cadenas, A. F., Moreno-Castilla, C., Costa, C. A., & Madeira, L. M. (2007). Azo-dye Orange II degradation by heterogeneous Fenton-like reaction using carbon-Fe catalysts. *Applied Catalysis B: Environmental*, 75(3-4), 312-323. <https://doi.org/10.1016/j.apcatb.2007.05.003>
- Rossi, A. F., Martins, R. C., & Quinta-Ferreira, R. M. (2014). Composition effect of iron-copper composite catalysts in the fenton heterogeneous process efficiency and cooxidation synergy assessment. *Industrial and Engineering Chemistry Research*, 53(40), 15369-15373. <https://doi.org/10.1021/ie501193x>
- Sánchez-Sánchez, C., González-González, A., Cuadros-Salcedo, F., & Cuadros-Blázquez, F. (2020). Two-phase Olive mill waste: A circular economy solution to an imminent problem in Southern Europe. *Journal of Cleaner Production*, 274. <https://doi.org/10.1016/j.jclepro.2020.122789>
- Sani, S., Dashti, A. F., & Adnan, R. (2020). Applications of Fenton oxidation processes for decontamination of palm oil mill effluent: A review. *Arabian Journal of Chemistry*, 13(10), 7302-7323. <https://doi.org/10.1016/j.arabjc.2020.08.009>
- Sellers, R. M. (1980). Spectrophotometric determination of hydrogen peroxide using potassium titanium(IV) oxalate. *The Analyst*, 105(1255), 950-954. <https://doi.org/10.1039/an9800500950>
- SIMDOURO-Grupo Águas de Portugal. (n.d.). *INTERNAL REGULATION OF THE CONDITIONS FOR THE INFLOW OF WASTEWATER TO THE INFRASTRUCTURE OF SIMDOURO - MULTI-TOWN SANITATION SYSTEM OF THE PORTO AREA*.
- Talinli, I., & Anderson, G. K. (1992). Interference of hydrogen peroxide on the standard cod test. *Water Research*, 26(1), 107-110. [https://doi.org/10.1016/0043-1354\(92\)90118-N](https://doi.org/10.1016/0043-1354(92)90118-N)
- Tatibouët, J. M., Guélou, E., & Fournier, J. (2005). Catalytic oxidation of phenol by hydrogen peroxide over a pillared clay containing iron. Active species and pH effect. *Topics in Catalysis*, 33(1-4), 225-232. <https://doi.org/10.1007/s11244-005-2531-3>
- The Council of the European Communities. (1976). *Council Directive: on pollution caused by certain*

dangerous substances discharged into the aquatic environment of the Community. Official Journal of the European Community. <http://eur-lex.europa.eu/legal-content/EN/TXT/PDF/?uri=CELEX:31976L0464&from=EN>

- Xu, M., Wu, C., & Zhou, Y. (2020). Advancements in the Fenton Process for Wastewater Treatment. *Intech, tourism*, 12. <https://www.intechopen.com/books/advanced-biometric-technologies/liveness-detection-in-biometrics>
- Zazo, J. A., Casas, J. A., Mohedano, A. F., & Rodríguez, J. J. (2006). Catalytic wet peroxide oxidation of phenol with a Fe/active carbon catalyst. *Applied Catalysis B: Environmental*, 65(3-4), 261-268. <https://doi.org/10.1016/j.apcatb.2006.02.008>
- Zazo, J. A., Pliego, G., Blasco, S., Casas, J. A., & Rodriguez, J. J. (2011). Intensification of the Fenton process by increasing the temperature. *Industrial and Engineering Chemistry Research*, 50(2), 866-870. <https://doi.org/10.1021/ie101963k>
- Zazouli, M. A., & Shahmoradi, M. (2019). Efficiency of fenton process in olive oil mill wastewater treatment. *Journal of Mazandaran University of Medical Sciences*, 29(176), 116-125. <http://jmums.mazums.ac.ir/article-1-13022-en.html>
- Zhang, M. hui, Dong, H., Zhao, L., Wang, D. xi, & Meng, D. (2019). A review on Fenton process for organic wastewater treatment based on optimization perspective. *Science of the Total Environment*, 670, 110-121. <https://doi.org/10.1016/j.scitotenv.2019.03.180>
- Zhang, X., Geng, Z., Jian, J., He, Y., Lv, Z., Liu, X., & Yuan, H. (2020). Potassium ferrite as heterogeneous photo-fenton catalyst for highly efficient dye degradation. *Catalysts*, 10(3). <https://doi.org/10.3390/catal10030293>

Appendix A

A.1 Phenolic compounds calibration curves

To determine the concentration of each phenolic compound in solution during the experiments by HPLC, calibration curves were constructed and validated using individual standard solutions with various initial concentrations (in the range of 5 to 100 mg L⁻¹). The correspondent peak areas for each concentration were plotted as shown in figures A.1 to A.4.

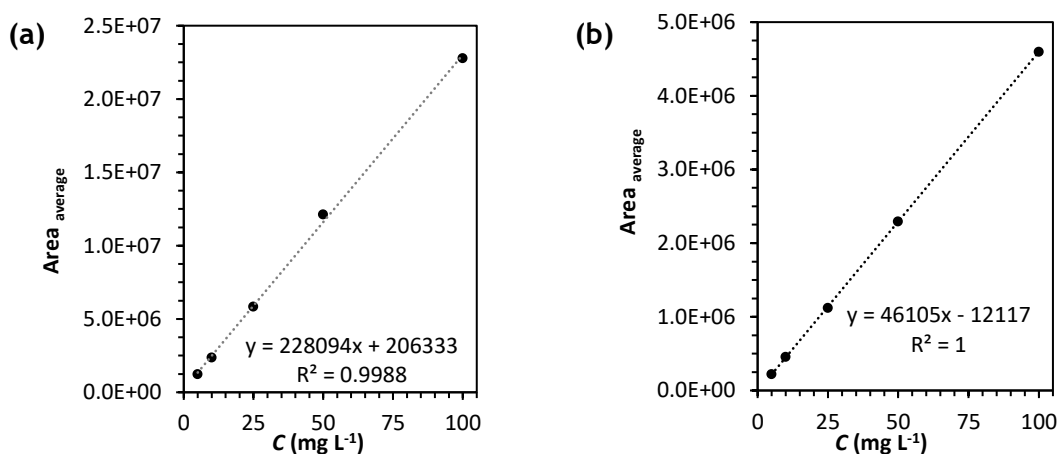


Figure A.1 Calibration curves for (a) gallic acid and (b) tyrosol.

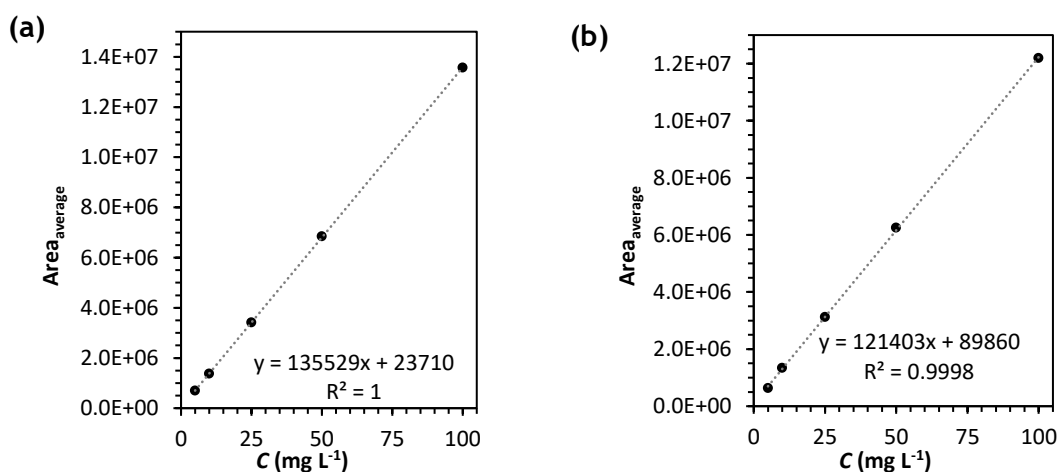


Figure A.2 Calibration curve for (a) 4-hydroxybenzoic acid and (b) protocatechuic acid.

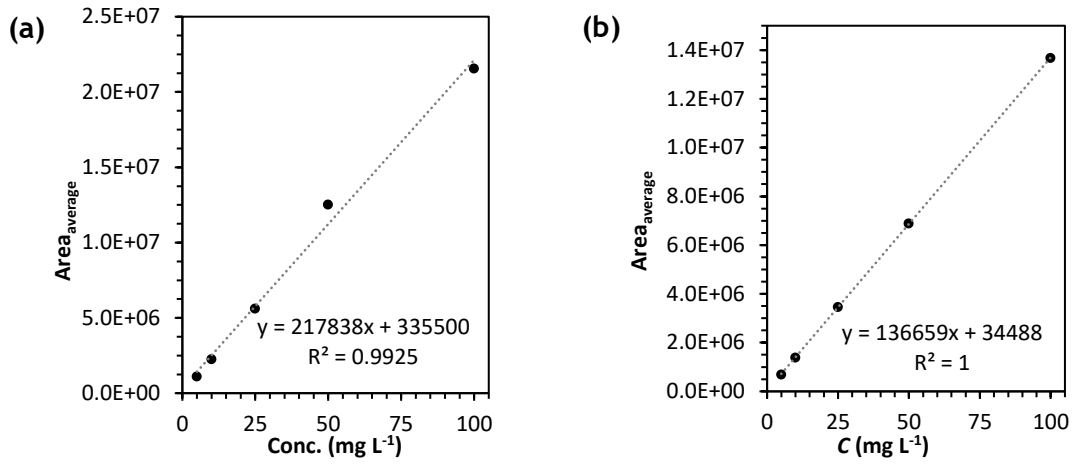


Figure A.3 Calibration curve for (a) caffeic acid and (b) vanillic acid.

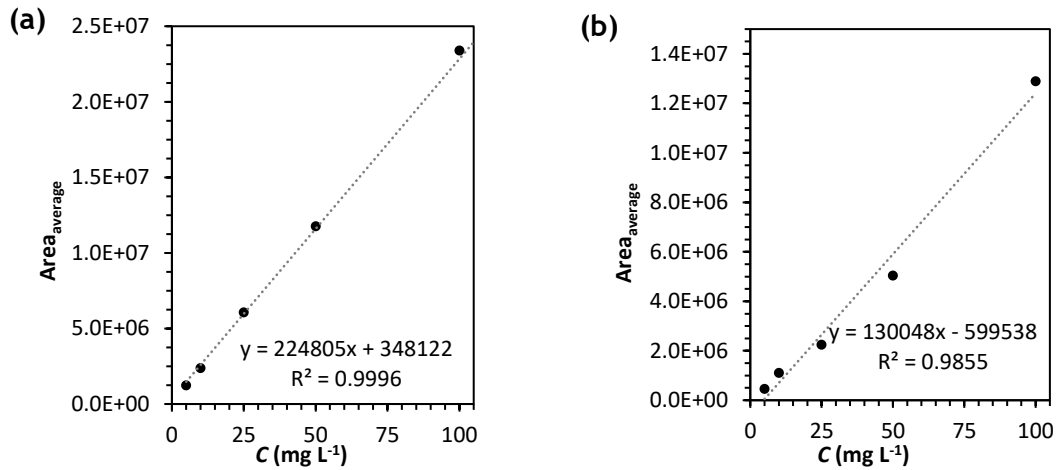


Figure A.4 Calibration curve for (a) syringic acid and (b) veratric acid.

A.2 H₂O₂ solution and calibration curve

In order to calculate the amount of hydrogen peroxide present in the solution, first it is necessary to obtain a calibration curve. To construct the calibration, curve several standard H₂O₂ solutions with concentrations ranging from 5 mg L⁻¹ to 100 mg L⁻¹ were prepared. Following the colorimetric method developed by Sellers, the corresponding absorbance values (at $\lambda = 400$ nm) were measured as shown in figure A.5.

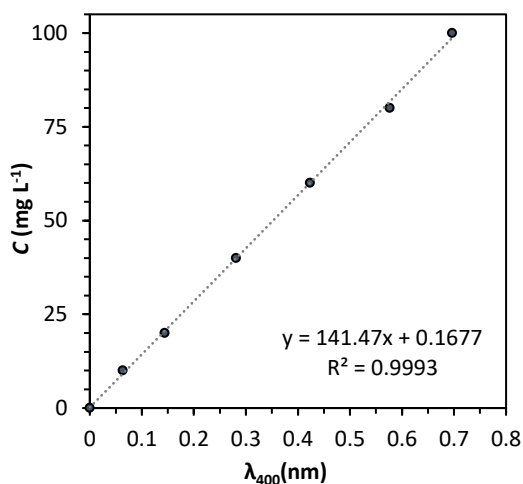


Figure A.5 Calibration curve of H₂O₂ at 400 nm for different concentrations.

Using the calibration curve, it is possible to calculate the H₂O₂ concentration values for each sample using equation A.1.

$$C = m \cdot x + b \quad (\text{Equation A. 1})$$

C is the calculated concentration, m is the slope, x is the measured absorbance, and b is the intercept. Since the correlation coefficient (R^2) is close to 1, the calibration curve is appropriate, and the obtained values are statistically correct.

A.3 Folin-Ciocalteu method

The Folin-Ciocalteu reagent was selected to determine the total phenolic content (TPh) of the real OMW effluent. Since it is a colorimetric method, a calibration curve and the respective linear regression are required to obtain TPh concentrations. For this purpose, gallic acid (GA) is used as a standard and concentrations are expressed as GA equivalents ($\text{mg}_{\text{CAeq}}/\text{L}$). Standard solutions in the 5 - 200 mg L^{-1} were prepared, and corresponding absorbance measured at $\lambda = 765 \text{ nm}$, as shown in figure A.6.

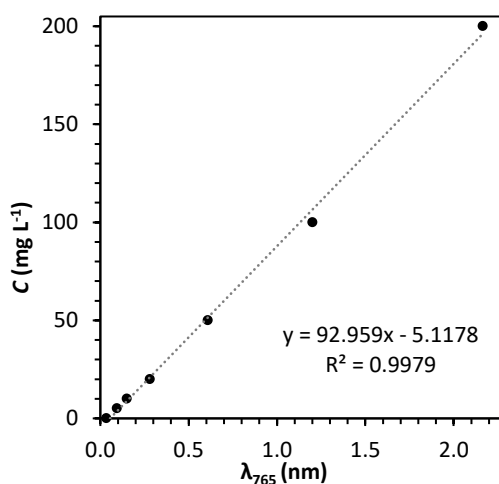


Figure A.6 Calibration curve for the Folin-Ciocalteu method.

After attaining the calibration curve, it is possible to calculate the concentration of phenolic compounds knowing the values of the slope and intersection. Since the correlation coefficient is close to the maximum then the calibration curve is appropriate. The TPh values were obtained using equation A.2.

$$C_{TPh} = m * \lambda + b \quad (\text{Equation A.2})$$

A.4 COD measurements: H₂O₂ interference

After attaining the COD values of each OMW sample, it is necessary to assemble a calibration curve and the correspondent linear regression to calculate the real amount of organic components present after the oxidation. Several authors have been studying the interference of the H₂O₂ in COD values (Kang et al., 1999; Talinli & Anderson, 1992) so it is necessary to evaluate this interference in order to obtain correct values. To do so it is prepared standard solutions with different concentrations of H₂O₂ and measured the correspondent COD values at 620 nm, see table A.1.

Table A.1 H₂O₂ concentration, absorbances and COD values at 620nm for the COD calibration curve.

H ₂ O ₂ concentration (g L ⁻¹)	λ ₆₂₀ (nm)	COD (mg L ⁻¹)
0.25	0.049	107
0.50	0.097	236
0.75	0.134	335
1.0	0.189	482

After acquiring the COD values, the calibration curve is plotted, and the linear regression obtained so it is possible to attain the concentration of the organic compounds. The calibration curve is attained by representing the COD values against the H₂O₂ concentration, see figure A.7.

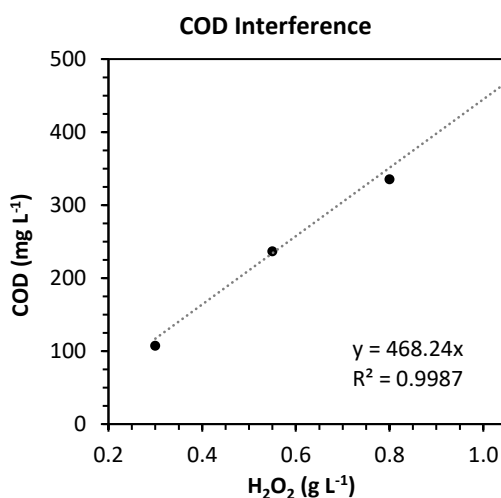


Figure A.7 Calibration curve for COD measures at 620 nm with H₂O₂ discount.

The amount of organic load was calculated using the mean of 3 COD readings subtracted to a blank value, afterwards the COD values are calculated using equation A.3.

$$COD = 2666.9 * COD_{average} - 22.317 \quad (\text{Equation A.3})$$

Since the samples were diluted before the COD measures, it is necessary to include the dilution factor (D), see equation A.4.

$$COD_{corrected} = COD * D \quad (\text{Equation A.4})$$

The final value of COD is given after discounting the H₂O₂ interference, for that, it is necessary to calculate the correspondent interference using equation A.5.

$$H_2O_2 \text{ interference} = \frac{[H_2O_2] * m}{D} \quad (\text{Equation A.5})$$

The final value of COD is giving by equation A.6.

$$COD_{Final} = COD_{corrected} - H_2O_2 \text{ interference} \quad (\text{Equation A.6})$$

A.5 Iron weight percentage and Fe leaching (%)

In order to obtain the iron weight percentage in the catalyst, it was necessary to perform an acid digestion, and use atomic absorption spectrometry (ASS) analysis. To obtain the values, first it is calculated the concentration of iron in each sample, see equation A.7.

$$C_{Fe} = C_{ASS} * D \quad (\text{Equation A.7})$$

Then, it is possible to calculate the weight (mg), and % of iron in weight (wt.) using equations A.8 and A.9.

$$m_{Fe} = C_{Fe} * V \quad (\text{Equation A.8})$$

$$wt. (\%) = \frac{m_{Fe}}{m_{sample}} * 100 \quad (\text{Equation A.9})$$

The amount of Fe leached is calculated considering the percentage of iron in each catalyst, previously obtained, and the volume of solution used. In tables A.2 and A.3, are presented the correspondent values of iron weight (wt.%) and Fe leached (%) into the solution for the different catalyst's particle sizes.

Table A.2 Concentrations, mass, and dilution factor for each catalyst series and the correspondent iron weight in mass percentage.

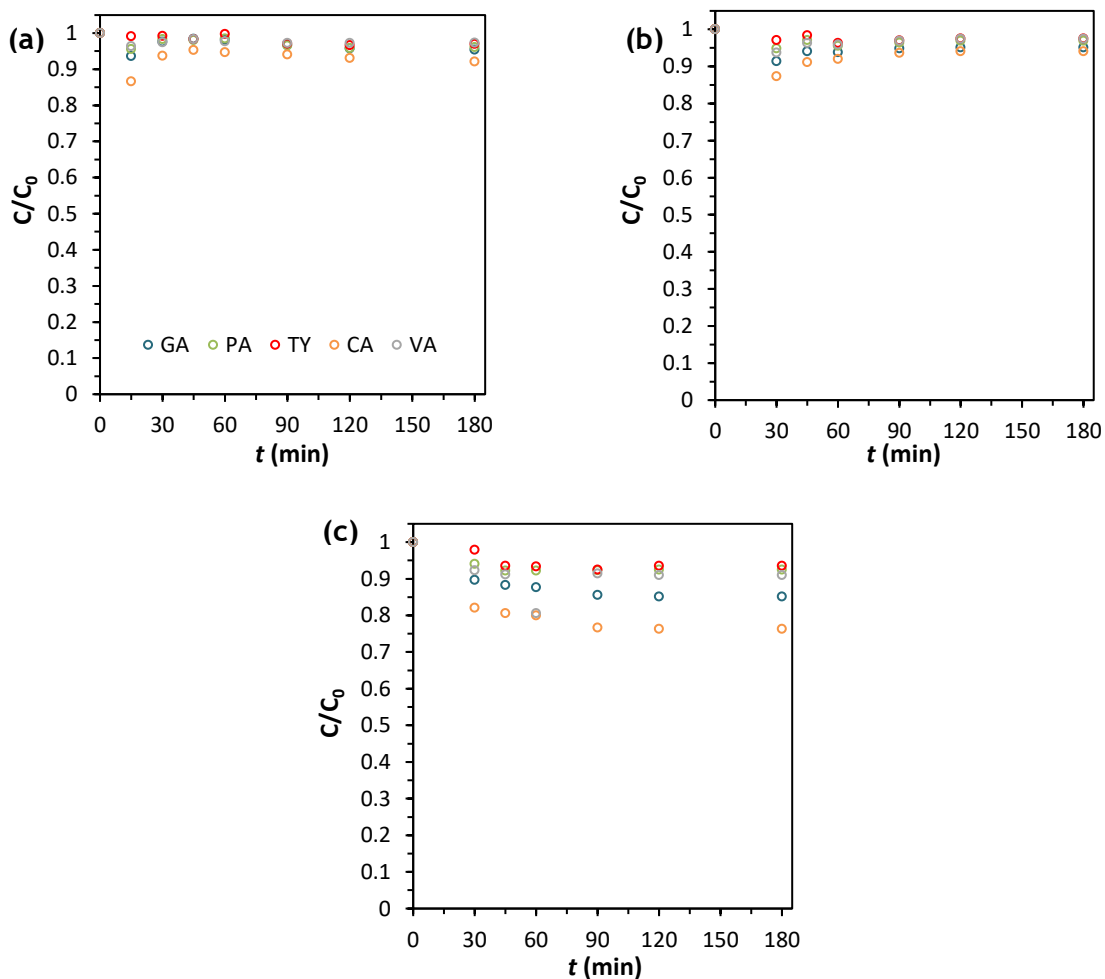
Particle Size (mm)	m _{sample} (mg)	[Cat] (mg L ⁻¹)	[AAS] (mg L ⁻¹)	Dilution Factor (D)	[Fe] (mg L ⁻¹)	m _{Fe} (mg)	wt. (%)
0.80	49.8	1992	2.29	50.0	114.4	2.86	5.74
0.45-0.80	50.0	2000	1.64	51.7	84.9	2.12	4.25
0.25	50.1	2004	1.92	50.0	96.0	2.40	4.79

Table A.3 Iron weight, mass, concentration, and iron leached in each catalyst.

Particle Size (mm)	wt. (%)	m _{Fe} (mg)	[Fe] (mg L ⁻¹)	[AAS] (mg L ⁻¹)	Fe _{leached} (%)
>0.80	5.74	4.31	28.71	0.409	1.42
0.45-0.80	4.25	3.19	21.25	1.64	1.28
<0.25	4.79	3.59	23.95	0.573	2.39
[0.5 g L ⁻¹]	5.74	4.31	28.71	0.409	1.42
[1.5 g L ⁻¹]	5.74	4.31	28.71	0.520	1.81
[2.5 g L ⁻¹]	5.74	4.31	28.71	2.29	7.97

Appendix B - TPh, TOC removals and H₂O₂ consumption for synthetic solutions

B.1 Influence of catalyst's particle size



CA - Caffeic acid; VA - Vanillic acid; GA - Gallic acid; TY - Tyrosol; PA - Protocatechuic acid

Figure B.1 Removal of phenolic compounds (C/C_0) over time during the adsorption process using catalysts with different particle sizes (d_p) (a) $0.80 < d_p < 1.0$ mm, (b) $0.45 < d_p < 0.80$ mm, and (c) $d_p < 0.25$ mm. Experimental conditions: SYNTHETIC-1 solution, $[CAT] = 0.5 \text{ g L}^{-1}$, $[H_2O_2] = 0.5 \text{ g L}^{-1}$, $T = 25 \text{ }^\circ\text{C}$, and $\text{pH} = 3.6$.

B.2 Influence of solution's composition

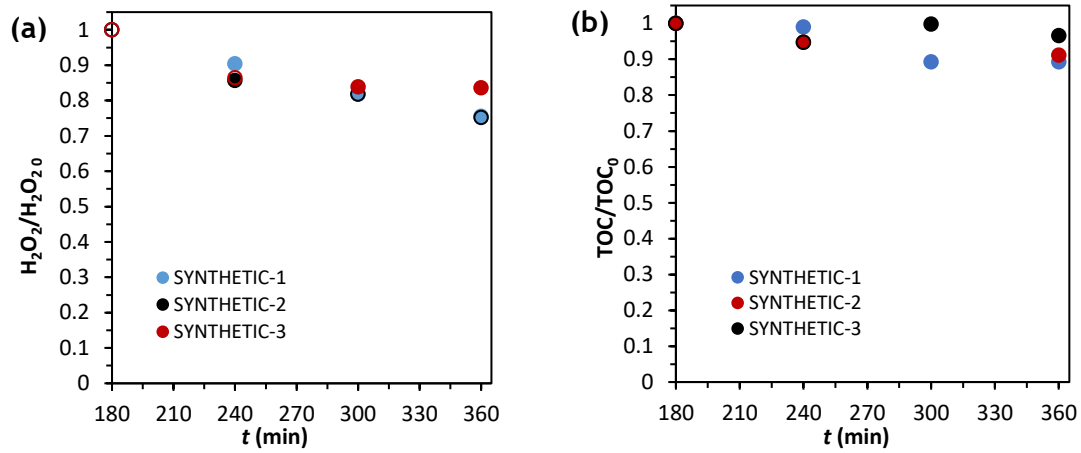
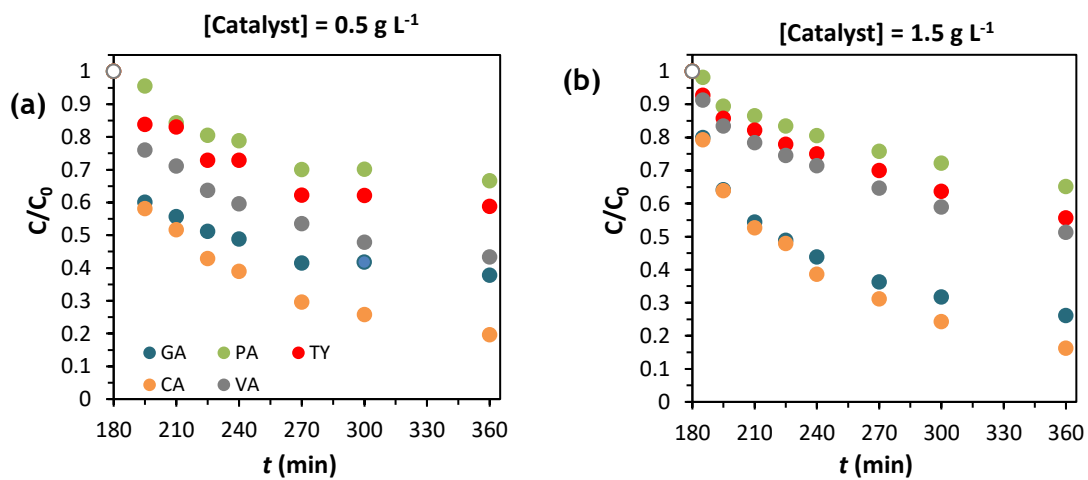
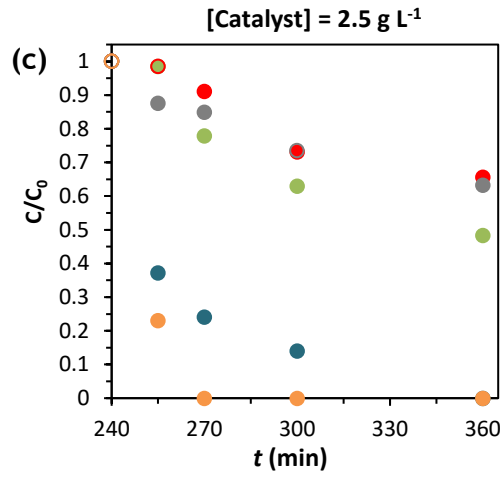


Figure B.2 a) Consumption of oxidant and (b) TOC removal during the catalytic process using different solution's compositions. Experimental conditions: $[CAT] = 0.5 \text{ g L}^{-1}$, $0.80 < d_p < 1.0 \text{ mm}$, $[H_2O_2] = 0.5 \text{ g L}^{-1}$, $T = 25 \text{ }^\circ\text{C}$, and $pH = 3.6 - 3.8$.

B.3 Influence of catalyst load





CA - Caffeic acid; VA - Vanillic acid; GA - Gallic acid; TY - Tyrosol; PA - Protocatechuic acid

Figure B.3 Removal of phenolic compounds over time using different catalyst concentrations. Experimental conditions: SYNTHETIC-1 solution, $0.80 < d_p < 1.0$ mm, $[H_2O_2] = 0.5$ g L⁻¹, $T = 25$ °C, and $pH = 3.6$.

Appendix C - TPh, TOC, COD removals and H₂O₂ consumption for real olive mill wastewaters

C.1 Influence of catalyst load

Table C.1 TPh, TOC, COD removals, and H₂O₂ consumption for real OMW using (a) 0.5 g L⁻¹, (b) 1.0 g L⁻¹, (c) 1.5 g L⁻¹ of catalyst with [H₂O₂] = 0.5 g L⁻¹.

(a)

t (min)	TPh (mg L ⁻¹)	TOC (mg L ⁻¹)	COD (mg L ⁻¹)	H ₂ O ₂ (nm)
0	79.9	563.2	1247.9	539.3
60	38.1	550	-	-
90	-	-	-	450.1
120	-	545.2	-	-
180	-	-	-	346.9
240	37.1	537	-	-
300	-	-	-	-
360	35.0	520.0	999.9	298.9

(b)

t (min)	TPh (mg L ⁻¹)	TOC (mg L ⁻¹)	COD (mg L ⁻¹)	H ₂ O ₂ (nm)
0	75.4	586.4	1435	529.4
60	48.0	563.9	-	505.3
120	-	555.4	-	447.3
180	-	-	1176.8	372.3
240	39.8	552.7	-	-
300	-	-	-	331.3
360	36.0	552.7	1173.2	280.5

(c)

t (min)	TPh (mg L ⁻¹)	TOC (mg L ⁻¹)	COD (mg L ⁻¹)	H ₂ O ₂ (nm)
0	75.0	534.7	1372	458.6
60	46.9	503.1	1123	345.4
120	-	469.8	-	286
180	-	-	1120	273.3
240	42.8	469.2	-	-
300	-	-	-	171.4
360	37.6	464.5	1044.2	168.6

C.2 Influence of temperature

Table C.2 TPh, TOC, COD removals, and H₂O₂ consumption for real OMW at (a) T = 25 °C, (b) T = 50 °C and (c) T = 75 °C using [CAT] = 0.5 g L⁻¹ and [H₂O₂] = 0.5 g L⁻¹.

(a)

t (min)	TPh (mg L ⁻¹)	TOC (mg L ⁻¹)	COD (mg L ⁻¹)	H ₂ O ₂ (nm)
0	79.9	563.2	1247.9	539.3
60	38.1	550	-	-
90	-	-	-	450.1
120	-	545.2	-	-
180	-	-	-	346.9
240	37.1	537	-	-
300	-	-	-	-
360	35.0	520.0	999.9	298.9

(b)

t (min)	TPh (mg L ⁻¹)	TOC (mg L ⁻¹)	COD (mg L ⁻¹)	H ₂ O ₂ (nm)
0	71.5	566.9	1312.2	479.8
30	44.2	551.2	1230.8	414.8
60	40.8	531.4	1209.7	383.6
120	37.1	-	1208	281.8
180	-	-	1205.1	223.8
240	27.0	504.8	1153.9	158.7
270	26.6	486.3	1153.3	123.3

(c)

t (min)	TPh (mg L ⁻¹)	TOC (mg L ⁻¹)	COD (mg L ⁻¹)	H ₂ O ₂ (nm)
0	87.4	592.9	1273	477
15	56.1	519.8	1059	-
30	54.7	509	878.5	317.2
45	17.7	431.5	857.5	270.5
60	11.1	397.4	701.5	154.5
90	9.1	351	617.1	32.8
120	6.5	348.2	532.5	25.7